

LUÍS ANTÓNIO DE MATOS BARRETO

Response to simulated El Niño stress by *Macrocystis pyrifera*



2017

LUÍS ANTÓNIO DE MATOS BARRETO

Response to simulated El Niño stress by *Macrocystis pyrifera*

Dissertation for Master's degree in Marine Biology

Advisors:

Ester Serrão
Gareth Pearson

Co-advisor:

Lydia Ladah



2017

“Response to simulated El Niño stress *in Macrocytis pyrifera*”

Declaração de autoria de trabalho

Declaro ser a autora deste trabalho, que é original e inédito. Autores e trabalhos consultados estão devidamente citados no texto e constam da listagem de referências incluída.

Luís António de Matos Barreto

Direitos de cópia ou Copyright:

© Luís Barreto:

A Universidade do Algarve tem o direito, perpétuo e sem limites geográficos, de arquivar e publicitar este trabalho através de exemplares impressos reproduzidos em papel ou de forma digital, ou por qualquer outro meio conhecido ou que venha a ser inventado, de o divulgar através de repositórios científicos e de admitir a sua cópia e distribuição com objetivos educacionais ou de investigação, não comerciais, desde que seja dado crédito ao autor e editor.

Acknowledgements

I want to thank my supervisors Gareth Pearson, Ester Serrão and Lydia Ladah for giving me this incredible opportunity and always being there to support and guide me.

Dr. Zertuche for his hospitality and wise advise.

Mariana-Sanchez for all the help, patience and friendship. Could not have been done without your help!

All the 2015 Ice team members and voluntaries that worked countless nights without sleep.

BEE lab. team, Rita (she came to the rescue!), Neusa, Licinia, Neiva, Tania and Cristina.

Daniel Reed for all the sampling, shipping and the constructive comments and ideas during our project.

Jorge Assis for building our climatologies.

All the volunteers in Portugal that helped during the sporophytes growth.

Cristovão Nunes for all the tips in the tanks design and setup.

To my Family and friends for all the love and support, in special to my mother for always being there for and with me.

All the ones that should be here, you know.

And to Mafalda for being that special reason why we grow together, our new adventure is already here!!

Abstract

Compelling evidence on environmental and species distribution changes due to global climate change have greatly increased over the last decades and extreme events like marine heatwaves (MHWs) (concurrent high temperature and low nutrient) are increasing in frequency, duration and intensity. The giant kelp, *Macrocystis pyrifera* (L.) C.A. Agardh forms dense marine forests serving as a foundation species in ecosystems that are of great ecological and economic importance. Thus, the objective of this study was to test for evidence of local adaptation to conditions representative of MHWs stress in the field on a regional level, encompassing areas with different oceanographic regimes and genetic groups. Adult blades from two depths and four regions of the Northeast Pacific were exposed to simulated nutrient and thermal stress conditions. The results clearly showed that *M. pyrifera* populations at the southernmost limit displayed greater thermal tolerance in their photosynthetic physiology. Compared to the other regions, surface blades from the South suffered reduced impact on the photosynthetic apparatus, with F_v/F_m values at 24°C 15.5% higher than the regional mean. Thermally-sensitive parameters governed mainly by enzymatic processes ($rETR_{max}$ and Ek) were unaffected over the 15 - 24°C range in the southernmost region, suggesting adaptation to local environmental conditions. Amongst the bottom blades collected at depth, photosynthetic responses to stress were rather similar among different regions. The F1 juvenile generation grown *in vitro* from parental source material did not exhibit a significant reductions in F_v/F_m under the moderate stress temperature used (21°C), but $rETR_{max}$ and Ek remained significantly higher in the Southern regions. Consistently poor photosynthetic responses to thermal stress were observed in the North-Center region (Santa Barbara) in all experiments, suggesting genetically-based fitness reduction. Our results also highlighted the need for further research on the synergistic effects of low nutrients availability and high thermal stress considering different life stages of *M. pyrifera*.

Key-words: Giant kelp, foundation species, climate change, thermal stress, local adaptation

Resumo

Evidências científicas de alterações no ambiente e distribuição de espécies devido a mudanças climáticas de caracter global, tem aumentado largamente nas últimas décadas. Eventos como as ondas de calor marinhas, têm aumentado a sua frequência (em cerca de 38%), duração e intensidade, ameaçando vários ecossistemas marinhos como recifes de coral, pradarias marinhas e florestas marinhas, assim com espécies de grande relevância económica. Espécies como as lagostas e as amêijoas foram afetadas através da redução do habitat e por *stress* térmico, o que resultou num aumento da mortalidade, na redução do tamanho dos indivíduos e da sua taxa de reprodução.

O Kelp gigante, *Macrocystis pyrifera* (L.) C.A. Agardh é o kelp com maior distribuição nos oceanos que forma extensas florestas marinhas, com uma canópia densa na superfície resultando numa grande produção primária a qual alimenta diretamente organismos herbívoros mas maioritariamente detritívoros. Devido a sua densidade e dimensão, as florestas de *M. pyrifera* são capazes de alterar as condições ambientais locais, nomeadamente reduzindo correntes e luz, criando um habitat heterogéneo, abrigando um grande número de espécies. Assim, funciona como uma espécie fundadora do ecossistema apresentando grande relevância ecológica e económica.

A fotossíntese é influenciada pela temperatura que regula as taxas de reações e movimentos de solutos dentro das células das algas tendo sido utilizada com sucesso noutros estudos, para quantificar o efeito de aumento de temperatura em kelps. Um dos métodos mais comuns para medir respostas fotossintéticas em eco-fisiologia é o fluorómetro (PAM), pois é capaz de determinar eficientemente as taxas fotossintéticas em laboratório e também no campo.

A utilização de técnicas de deteção remota como boias e satélites em estudos oceanográficos, permite obter dados a uma grande escala e com grande regularidade possibilitando a análise de padrões e fatores relevantes como por exemplo oscilações da temperatura da superfície do mar (SST) ou movimentos da camada de gelo polar. Esta técnica pode também ser utilizada para gravar eventos a uma escala temporal mais curta, como *blooms* de fitoplâncton e processos de afloramento costeiro. Dado que a macroalga *M. pyrifera* forma uma canópia densa à superfície da água do mar, a utilização de dados de satélite (capazes de detetar a fluorescência da Clorofila *a*). Esta ferramenta tornou-se

essencial na análise da distribuição, padrões sazonais de crescimento e correlação das florestas de kelp gigante com fenômenos ambientais como furacões ou eventos como o El Niño. A análise de climatologias, resumos de uma ou mais variáveis (SST ou Clorofila *a*) em escalas temporais grandes, utiliza modelos de fluxos atmosféricos e oceanográficos com enormes bases de dados e capacidade de processamento dos mesmos (como por exemplo o sistema de reanálise de dados oceanográficos ORAS4). Estes aumentam a quantidade e qualidade dos dados utilizáveis para estudar os fatores ambientais que afetam a espécie em estudo e permitem a criação de cenários de hipotéticos de alterações na distribuição destas espécies.

O objetivo deste estudo foi procurar evidências de adaptação local a condições representativas de stress relacionado com ondas de calor marinhas (temperaturas altas e baixa concentração de nutrientes) a um nível regional numa área que engloba regimes oceanografias diferentes, assim como diferentes grupos genéticos.

Em 2015, lâminas de *M. pyrifera* adultas amostradas a duas profundidades e provenientes de quatro regiões do Pacífico Noroeste foram expostas a um gradiente de água do mar a 3 temperaturas (15, 20 e 24°C) e nutrientes (meio não enriquecido e enriquecido com Provasoli (PES)) replicados ($\times 3$), simulando condições similares fenômenos com o El Niño. Tanques de 30L contendo água do mar filtrada foram equipados com termostatos para regular a temperatura, bombas de circulação de água e aparelhos de registo de temperatura para registar o seu perfil. As condições de cultura foram: salinidade a 35ppm, ciclos de 14:10 luz:escuro a $80 \mu\text{E} \cdot \text{m}^{-2} \cdot \text{s}^{-1}$ e os tratamentos com adição de nutrientes foram enriquecidos com $20 \text{ mL} \cdot \text{L}^{-1}$ PES.

Os resultados das experiências revelaram, com grande expressividade, que as populações de kelp gigante do limite sul da distribuição geográfica no hemisfério norte, expressavam na sua resposta fotossintética uma maior tolerância ao *stress*. Comparada com as outras regiões, as lâminas da superfície da região Sul, demonstraram uma menor perturbação no aparelho fotossintético com os valores do parâmetro F_v/F_m 15.5% superiores à média regional, nos tratamentos a 24°C. Também na região Sul, os parâmetros relacionados com os processos fotossintéticos de enzimas termo sensíveis ($rETR_{max}$ e Ek) foram mais elevados a 24°C comparativamente com os tratamentos a 20°C, o que não sucedeu nas outras regiões. Nas lâminas amostradas junto ao fundo, as repostas fotossintéticas ao *stress* apresentaram maior semelhança entre regiões. Esporófitos juvenis crescidos em

laboratório, a partir do tecido reprodutivo recolhido nas mesmas populações amostradas para as lâminas adultas, não exibiram uma redução significativa do parâmetro F_v/F_m , provavelmente devido à temperatura máxima utilizada (21°C) a qual não foi suficientemente alta para causar *stress* térmico. No entanto, os parâmetros $rETR_{max}$ e E_k foram significativamente mais altos na região Sul. A região Norte-Centro (Santa Barbara, Califórnia) revelou os níveis mais baixos de resposta fotossintética ao *stress* em todas as experiências, incluindo nos esporófitos F1. Este facto aponta para uma possível redução de *fitness* devido a fatores genéticos. Os nossos resultados realçam também a necessidade de futuras investigações nos efeitos sinérgicos de baixa disponibilidade de nutrientes, associada a elevadas temperaturas considerando diferentes etapas no ciclo de vida de *M. pyrifera*.

Palavras-chave: Kelp, espécies, espécies estruturais, alterações climáticas, *stress* térmico, adaptação local

Contents

Introduction	1
Objectives	5
Materials and Methods	6
Common-garden experiment comparing adult blades (Experiment 1)	7
Oceanographic data	9
Effect of blade removal on physiological responses: Comparison of entire individuals vs excised blades (Experiment 2)	9
Control of environmental carry-over effects: Comparison of F1 generation juvenile sporophytes (Experiment 3)	10
Statistical analyses of experimental data	11
Results	13
Common-garden experiment comparing adult blades (Experiment 1)	13
Maximum quantum efficiency of PSII (F_v/F_m)	15
Light-limited photosynthetic rates (α)	16
Maximum electron transport rate ($rETR_{max}$)	16
Minimum saturating irradiance (E_k)	17
Oceanographic data	20
Comparison of entire individuals vs excised blades (Experiment 2)	22
Comparison of F1 generation juvenile sporophytes (Experiment 3)	25
Maximum quantum efficiency of PSII (F_v/F_m)	26
Light-limited photosynthetic rates (α)	26
Maximum electron transport rate ($rETR_{max}$)	26
Minimum saturating irradiance (E_k)	27
Discussion	28
Regional differences and potential for local adaptation	28
Thermal limits	30
Nutrient effects	32
Depth effects	33
Conclusions	34
References	35
Annexes	46

Abbreviations list

PAM fluorometer - Pulse Amplified Modulated fluorometer

RLC - rapid light curve

PSII - photosystem II

F_v/F_m - maximum quantum yield of PSII

ETR_{max} - maximum electron transport rate

$rETR_{max}$ - relative maximum electron transport rate

α - photosynthetic rate in light-limited region of RLC

E_k - minimum saturating irradiance

N – North

NC - North-Center

SC - South-Center

S - South

SW - seawater

RuBisCO - Ribulose-1,5-biphosphate carboxylase/oxygenase

ANOVA - Analysis of variance

GLM - Generalized Linear Models

ATP - adenosine triphosphate

V_{max} - maximum rate of enzymatic reaction

K_m - substrate affinity

ϕ_{PSII} - effective quantum yield of PSII

SST - sea surface temperature

Chl *a* - chlorophyll *a*

MHWs - Marine Heat Waves

PES - Provasoli Enriched Seawater

Introduction

Temperature is a major physical factor that defines the biogeographic distribution of species in the marine environment (Adey & Steneck, 2001; Poloczanska *et al.*, 2007; Wernberg *et al.*, 2016). Species range distributions are usually associated with a center where conditions are optimal and the edges where those conditions are no longer met (Lomolino *et al.*, 2006). Thermal limits occur where organisms can no longer tolerate continuous temperature conditions in the environment or their fluctuations (Garrabou *et al.*, 2009; Mohring *et al.*, 2014). While temperature change across the latitudinal range can be broadly contiguous, environmental factors such movement of air masses, ocean currents, hurricanes, upwelling and internal waves provide extreme complexity to the marine environment resulting in great spatial (from meters to hundreds of kilometers) and temporal (from hours to decades) thermal variability (Adey & Steneck, 2001).

Compelling evidence on environmental and species distribution changes due to global climate change have greatly increased over the last decades (Selig *et al.*, 2010; Wernberg *et al.*, 2012a; Rosenzweig & Neofotis, 2013; Caputi *et al.*, 2015). In a decadal review of scientific experiments related to climate change on marine organisms, Wernberg *et al.*, (2012b) found that virtually all experiments showed significant effects of stress related to increased temperatures. The frequency of high seawater temperature anomalies on nearshore ecosystems has increased 38% (Lima & Wethey, 2012) resulting in a mean temperature increase of 0.5-1°C (Hawkins *et al.*, 2003; Ridgway, 2007). Thus, extreme events like marine heatwaves (MHWs) characterized by a sudden significant increase of seawater temperature (but see Hobday *et al.*, 2016 for a recent detailed and hierarchical definition) are increasing in frequency, duration and intensity (Perkins, 2011; Hobday *et al.*, 2016). Examples of such events are the northern Mediterranean Sea marine heat wave (MHW) of 2003 (Garrabou *et al.*, 2009) or the 2014 positive temperature anomalies on the NE and equatorial Pacific that led to the extreme magnitude of the 2015/16 El Niño (Bond *et al.*, 2015; Levine & Mcphaden, 2016). MHWs are caused by the interaction of atmospheric and oceanographic processes that can encompasses different geographical (local, regional and global) and temporal (seasonal, yearly, decadal) scales (Trenberth, 2012; Hobday *et al.*, 2016).

These events are also affecting larger areas of the globe, threatening several marine ecosystems and key species (Lima & Wethey, 2012; Wernberg *et al.*, 2012a). Coral reefs are among the most sensitive ecosystems to anthropogenic related environmental changes (Halpern *et al.*, 2007) and recent extreme MHWs caused extensive bleaching and disease (Selig *et al.*, 2010; Smale & Wernberg, 2012b). Seagrass meadows (*e.g* *Posidonia oceanica*) also responded negatively after the two extreme MHWs events (2003 and 2006) in the Mediterranean when shoot mortality rates exceeded recruitment (Marbà & Duarte, 2010). Similar results were obtained in a laboratory experiment mimicking an ocean warming scenario on the seagrass *Zostera noltii*, with reduced photosynthetic performance and shoot density (Repolho *et al.*, 2017). Species with great economic relevance such as lobsters and scallops were also affected by the loss of habitat and direct thermal stress resulting in increased mortality, individual size reduction and reproductive rates (Mills *et al.*, 2013; Caputi *et al.*, 2015). Kelp forests and furoid beds have also registered negative effects caused by rising seawater temperature events on fundamental processes such as growth, reproduction, recruitment and resilience to disturbances (Ladah & Zertuche-González, 2007; Pearson *et al.*, 2009 ; Wernberg *et al.*, 2012a; Nicastro *et al.*, 2013; Jueterbock *et al.*, 2014; Mota *et al.*, 2015)

Photosynthesis is greatly influenced by temperature (Raven & Geider, 1988; Kirk, 2011) which regulates the rate of enzymatic reactions and solute movements within algal cells (Raven & Geider, 1988; Davison, 1991; Tamburic *et al.*, 2014) and has been successfully used to quantify the effects of temperature increase on kelps (Henkel & Hofmann, 2008; Wernberg *et al.*, 2010). While low temperatures reduce photosystem 2 (PSII) activity (Baker, 1991), high temperatures can result in protein denaturation and damage to the membrane systems of the photosynthetic apparatus (Daniel *et al.*, 1996). Thus, photosynthesis is often used as an indicator for algal stress response to temperature (Hurd *et al.*, 2014). As photosynthesis depends on the electron transport rate (ETR) in order to maintain cellular redox balance, metabolic homeostasis, and energy production (ATP) for the organism, this system is highly conservative in response to environmental (*e.g* temperature oscillations) and physiological changes (McDonald *et al.*, 2011). The other facet of photosynthesis, i.e., the Calvin cycle biochemical pathway through which inorganic carbon is fixed, is temperature dependent via effects on enzyme activity. Moderate temperature increase may enhance

photosynthesis by increasing maximum rates of enzymatic activity, beyond which further temperature increase may reduce the maximum rate (V_{\max}) and/or substrate affinity (K_m) of key enzymes such as RuBisCO. Limitation of photosynthetic process by inorganic carbon availability, carbonic anhydrase activity, diffusion and active transport of CO_2 across the chloroplast membrane may also occur at higher non-acclimated temperatures, contributing to declining photosynthetic rates (Davison, 1991).

One of the most commonly used methods to measure photosynthetic responses in ecophysiological research is the Pulse Amplified Modulated (PAM) fluorometer, as it can efficiently determine photosynthetic rates in laboratory and field conditions (Beer *et al.*, 1998; Ralph & Gademann, 2005; Roleda *et al.*, 2009; Terada *et al.*, 2016). These instruments generally have built-in software routines allowing efficient measurement of the maximum quantum yield of PSII (F_v/F_m), or the effective quantum yield of PSII under illumination (ϕ_{PSII}). ϕ_{PSII} together with information on illumination can be used to construct photosynthesis-irradiance curves, often as “rapid light curves” (RLCs) when illumination steps are given briefly (over several seconds). Declining F_v/F_m values imply a reduction in the maximum quantum yield of PSII photochemistry and therefore disturbance (short term photoacclimation) or damage to the photosynthetic apparatus (Lichtenthaler *et al.*, 2005). RLCs are a powerful tool that provide more detailed information on the maximum electron transport rate (ETR_{\max}), while the initial slope (α) of the RLC provides information about the relative efficiency of (PSII) photochemistry and the minimum saturating irradiance (E_k) reveal the dominance of photochemical quenching (Ralph & Gademann, 2005) and can be used as a photoacclimation indicator (Sakshaug *et al.*, 1997).

The giant kelp, *Macrocystis pyrifera* (L.) C.A. Agardh is the most widely distributed kelp taxon in the oceans, distributed through the northeast and southeast Pacific Ocean, in the southwest Atlantic Ocean, South Africa, Australia, New Zealand and also around most sub-Antarctic Islands (Graham *et al.*, 2007)). It has an heteromorphic life cycle in which the microscopic haploid gametophyte (male and female) alternates with a micro and macroscopic diploid sporophyte (Ladah & Zertuche-González, 2007; Graham & Halpern, 2008). *M. pyrifera* forms dense forests with thick canopy at the water surface where the majority of the sporophyte biomass is located (Nyman *et al.*, 1993; Graham *et al.*, 2007), resulting in high

net primary production (NPP) between 0.42 and 2.38 kg dry mass m⁻² y⁻¹ (Graham & Halpern, 2008). While this productivity feeds secondary production via direct grazing, most of this carbon follows the detrital pathway or is exported (Graham, 2004; Dean *et al.*, 1984). Due to their size, density and primary production, *M. pyrifera* forests are able to modify the local environmental conditions providing a heterogeneous habitat which can harbour a high number of species (Santelices & Ojeda, 1984; Graham, 2004). Therefore, this species serves as a foundation species in ecosystems that are of great ecological and economic importance (Lee *et al.*, 2009; Graham *et al.*, 2007; Byrnes *et al.*, 2011).

Due to the great importance of *M. pyrifera* as a structuring species in the Northeast Pacific, several studies have been conducted in recent years to understand the oceanographic processes affecting geographical range and genetic diversity of this species (Alberto *et al.*, 2010, 2011; Bell *et al.*, 2015; Johansson *et al.*, 2015). Across the broad latitudinal distribution of *M. pyrifera* in the Northeast Pacific, regionally heterogeneous environmental conditions raise the hypothesis that populations may be locally adapted. In general, adaptive genetic responses to the environment can occur on a time scale of years to hundreds of years (Crispo *et al.*, 2010). Examples of local adaptation to warmer and nutrient limited sea-water were already described for example in *Fucus serratus* (Jueterbock *et al.*, 2014); but see Pearson *et al.* (2009) for potential mal-adaptation in the same species) and coral reef endosymbionts (Howells *et al.*, 2012).

The use of remote sensing techniques such as oceanographic buoys and satellite data has greatly increased our knowledge of the marine environment as continuous observations allow for pattern analysis of relevant factors (*e.g.* sea surface temperature (SST) oscillations, ice shelf movements) and can record short-lived events (*e.g.* phytoplankton blooms, upwelling event) (Joint & Groom, 2000; Paolo *et al.*, 2015). Because *M. pyrifera* forms dense canopies at the water surface where most of the adult sporophyte biomass is located (Nyman *et al.*, 1993; Graham *et al.*, 2007) remote sensing by satellite data analysis has become a fundamental tool to assess kelp forest distribution, seasonal growth and correlation with environmental phenomena like hurricanes or El Niño events (North *et al.*, 1993; Graham *et al.*, 2007; Cavanaugh *et al.*, 2013). The analysis of climatologies (long-term summary of a single or multiple variables (*e.g.* SST, Chl *a*), ocean models, atmospheric forcing fluxes and

oceanographic observations by data integration in reanalysis systems (*e.g.* ocean reanalysis system ORAS4) provide improved quality controlled data sets that can be used to assess how environmental conditions affect target species and provide plausible scenarios concerning species range distribution shifts (Lee *et al.*, 2009 ; Balmaseda *et al.*, 2013)

Understanding the physiological responses of *M. pyrifera* to stress conditions will help to predict and possibly minimize reductions in range distribution. Although several studies have focused on the response of *M. pyrifera* to thermal stress (North & Zimmerman, 1984; Deyseher & Dean, 1986; Rothausler *et al.*, 2009; Xu *et al.*, 2013) a regional comparison between population responses that encompass areas with different oceanographic regimes and genetic groups has yet to be performed.

Objectives:

This study aims to test for evidence of local adaptation to conditions representative of heat waves in the field (*i.e.*, concurrent high temperature and low nutrient [inorganic N] stress) in populations of the giant kelp *Macrocystis pyrifera* at its southern limit in the northern hemisphere, in a region that encompasses distinct genetic groups and biogeographic thermal barriers, by comparing southern limit populations with those near the center of the range. This aim is approached by comparing ecophysiological responses of adult blades and F1 juvenile sporophytes from eight populations representing four distinct genetic regions.

Materials and Methods

In all tasks, the model used was the giant kelp *Macrocystis pyrifera* in the northeast Pacific between Baja California, Mexico and central California, U.S.A., an area covering around 1300 km of coastline that includes major biogeographic and thermal transition zones (Fig 1).

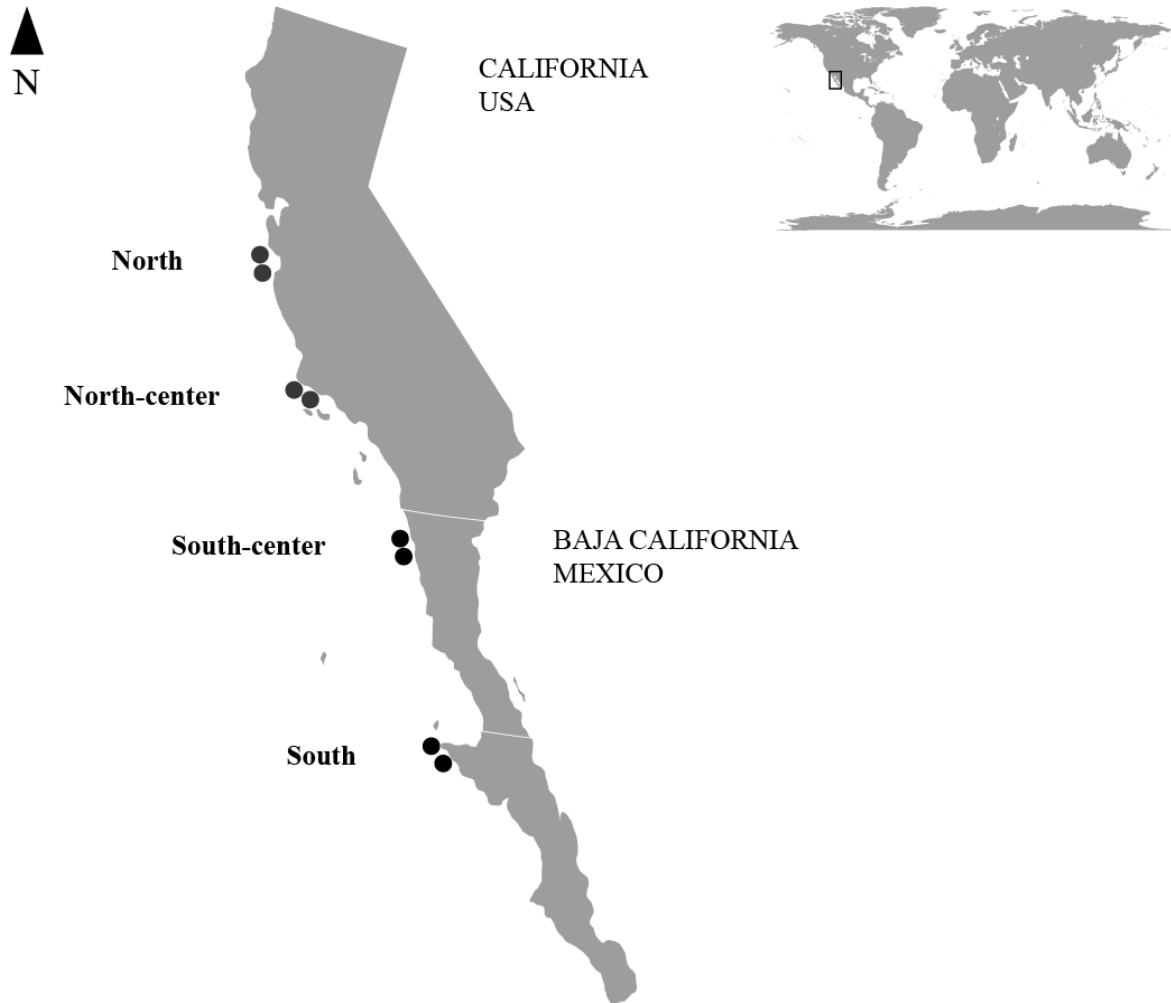


Figure1: Locations of the 8 populations (2 populations per region) sampled along the coast of California, USA (regions North, North-Center) and Baja California, Mexico (regions South-Center and South) (see Annex I for coordinates).

Common-garden experiment comparing adult blades (Experiment 1)

On June 18, 2015, adult *M. pyrifera* blades were simultaneously sampled by SCUBA diving from two populations within each of 4 regions in the northeast Pacific: 1) north (N) (Santa Cruz), 2) north-center (NC) (Santa Barbara) - both in the U.S.A, and 3) south-center (SC) (Ensenada) and 4) south (S) (Punta Eugenia) in Baja California, Mexico (Fig. 1, see Annex I for coordinates). Populations within a region were not very distant, but direct gene flow is expected to be low based on gaps in habitat continuity between populations (Alberto *et al.*, 2010). From each population, 54 blades were sampled from the surface and 54 blades near the bottom (at depth 15-20 m). In addition, 10 reproductive blades (sporophylls) were sampled for subsequent spore release. Blades were cleaned of epiphytes using paper towels, then packed in moistened paper towels and wrapped in aluminum foil. All blades were transported to Ensenada in cool-boxes packed with ice for the laboratory experiment and arrived within 24 h of collection. Samples from the Ensenada area were collected, prepared and stored in a similar way, to avoid transportation effects. Immediately on arrival at the laboratory, adult sporophyte blades were acclimated for 24h at 15 °C in 20 mL·L⁻¹ Provasoli seawater (SW) medium (PES; Provasoli, 1968) (Anderson, 2005).

The experimental design consisted of a replicated (×3) gradient of SW temperatures (15, 20, 24 °C) and nutrients (non-enriched or enriched SW with PES SW medium), simulating a range of environmental conditions including El Niño (Fig. 2).

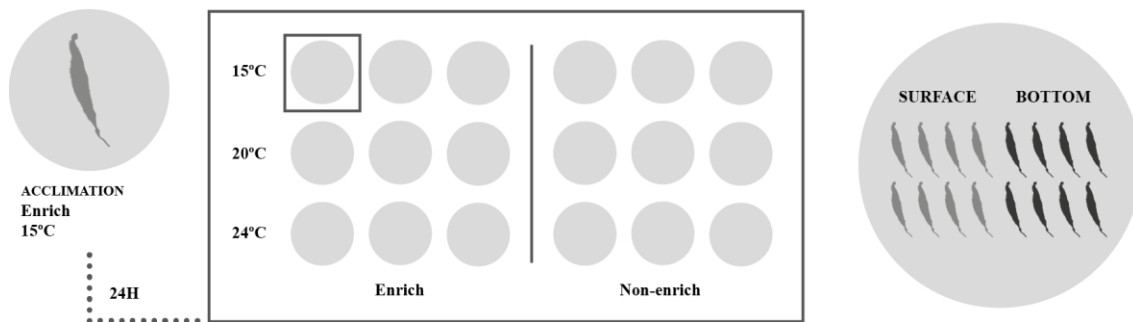


Figure 2: Experimental design. Acclimation for 24 h (15 °C, with nutrients) followed by transfer of blades to 3 replicates of each of 3 temperature treatment (15, 20, 24°C) with enriched and non-enriched seawater with PES. For each treatment condition (temperature and nutrients) a total of 3 blades per population (8 populations) x 2 depths (surface and bottom) were used.

Tanks containing 30 L filtered SW were equipped with thermostats to regulate temperature, pumps for water circulation and temperature loggers to record thermal profiles. Culture conditions were 14:10h light:dark cycle, $80 \mu\text{E} \cdot \text{m}^{-2} \cdot \text{s}^{-1}$ and treatments with nutrients were enriched with $20 \text{ mL} \cdot \text{L}^{-1}$ PES (Anderson, 2005) at 35 ppm salinity. Blades were placed inside large open-mesh (1 cm) bags to allow individual identification throughout the experiment while not significantly reducing light and water circulation reaching the blades. Three blades per population (and from each depth within that population) were placed in each treatment tank. The maximum temperature (24°C) was selected based on climatology analysis of the sites and thermal limits reported on literature (Hernandez-Carmona *et al.*, 2001; Ladah & Zertuche-González, 2007; Rothausler *et al.*, 2009)

The following physiological measurements were taken using a pulse amplified modulated (PAM) fluorometer (Diving PAM, Waltz, Germany) during the course of the experiment to allow a continuous assessment of the condition and stress responses of the algae: F_v/F_m (the maximum yield of photosystem 2 (PSII) photochemistry), and rapid light curves (photosynthesis versus irradiance curves from relative electron transport rates [rETR], calculated from PSII yield [$\Delta F/F_m$] at each irradiance level). F_v/F_m measurements and observation of blade condition were performed every 24h (starting at 12h) to determine if sampling was required due to tissue degradation (at higher temperatures). If so, rapid light curves were performed and tissue from each individual blade was sampled for gene expression. Tissue samples were flash-frozen in liquid nitrogen and later lyophilized in order to preserve tissue for RNA extraction. Diving PAM settings for the RLCs were the following: light curve intensity (LC-INT = 2), duration of each step (LC-WIDTH = 10seconds) and actinity light list for each step (1, 19, 45, 70, 94, 138, 219, 278 and 444). These settings allowed a plateau in the rETR curve to be reached (*i.e.*, saturated photosynthesis and in some cases photoinhibitory decline at the highest irradiance (Ralph & Gademann, 2005). RLC calibration was performed prior to the experiment using separate *M. pyrifera* blade samples.

Oceanographic data:

We analyzed local oceanographic features of each region prior to and during the sampling event for evaluation in light of the physiological results. Ocean temperature data were compiled on a daily basis at two depths (surface and 20 m) for each region. Data were derived from the Global Ocean Physics Reanalysis ECMWF ORAP5.0 (1979-2013), which uses a 3D model (NEMOVAR) with a bias correction scheme that combines satellite data and *in situ* measurements, for a spatial resolution of 0.25 degree x 75 depth levels (Balmaseda *et al.*, 2015; Zuo & Balmaseda, 2015; Zuo *et al.*, 2015). Bilinear interpolation was used to estimate the temperatures of each sampling site (e.g., Assis *et al.*, 2016). An anomalously warm event (heat wave) was defined similarly to Hobday *et al.* (2016) as five or more days of temperatures warmer than the 90th percentile of a historical baseline climatology, which in our study was considered for the period 1993-2015. The climatology was defined relative to the time of year, using all data within an 11-day window centered on the time of year from which the climatological threshold was calculated. The high percentile threshold (e.g. 90%) was used rather than an absolute value above the climatological value as the magnitude of variability across a range of timescales varies considerably by region (Hobday *et al.*, 2016).

Effect of blade removal on physiological responses: Comparison of entire individuals vs excised blades (Experiment 2)

In adult *Macrocystis pyrifera* sporophytes, photosynthesis is mostly performed at the canopy surface and the resulting products (mannitol and aminoacids) are translocated downwards to the youngest blades, meristems, holdfasts and sporophylls (Schmitz & Grant, 1979). As translocation in *M. pyrifera* is not fully understood, an experiment was designed in order to understand if individual responses to thermal stress (i.e. entire individuals, in this case small juveniles due to logistic constrains) differ from those of juvenile and adult excised blades. A total of 24 juveniles (smaller than 40 cm), 40 juvenile blades and 40 adult bottom blades from *M. pyrifera* sporophytes were collected from the Campo Kennedy population, in the South-center region. Two temperatures (16 and 24 °C) and nutrients concentration (non-enriched and enriched PES-enriched SW) were used with 2 × replicates per treatment. We used a lower

number of juveniles to minimize any population impact caused by the removal of young sporophytes. Culture conditions were replicated from the first experiment (see above) and F_v/F_m measurements were taken every 12h using the diving PAM fluorometer using the same settings as in the first experiment.

Control of environmental carry-over effects: Comparison of F1 generation juvenile sporophytes (Experiment 3)

A third experiment was designed in order to assess the ecophysiological responses of first filial (F1) generation sporophytes to thermal stress given a common growth history *in vitro*. Gametophytes developed from spores released from 10 fertile sporophylls per population used in Experiment 1 were grown vegetatively in 500 mL Erlenmeyer flasks with 4 mL·L⁻¹ of PES (Anderson, 2005) without iron, 35 ppm salinity, 20 $\mu\text{E} \cdot \text{m}^{-2} \cdot \text{s}^{-1}$ red light (LEE filters, #026 bright red) and aeration at 15°C.

On February 2017 a gametophyte mass from each population was manually separated into the smallest pieces possible using forceps. The fragments were seeded onto a spool of cotton filament and left for 2h in air under cool (15°C) and humid conditions to allow attachment. Seeded spools for each population were then placed separately into 20 L tanks with aerated seawater (SW) and weekly increasing concentrations of PES (6, 10, 15, 20 mL·L⁻¹) containing iron. Incubations proceeded under white light (20, 40 60 80 $\mu\text{E} \cdot \text{m}^{-2} \cdot \text{s}^{-1}$) and 14:10 h light:dark cycle. Seawater and tanks were changed/cleaned weekly to maintain optimal culture conditions. When sporophytes were ca. 1 cm length they were gently removed from the line using forceps and grown detached with aeration (see Westermeier *et al.*, 2006) in the same 20 L tanks. When sporophytes reached 6 to 10 cm they were transferred to the experimental setup. This constituted a temperature gradient (15, 17, 19 and 21°C) in PES-enriched SW, with 3 replicates of 5 sporophytes per final temperature. A 24 h ramp between each temperature increase was used to avoid excessive stress on the small juvenile sporophytes. All individuals were initially at 15°C, at 24 h all individuals were transferred to 17°C except the 15°C treatment, and so on up to 21°C.

Rapid light curves (RLCs) were performed every 24 h for 5 days using a diving PAM. Experimental conditions were: 10 L tanks with aeration, SW with 20 mL·L⁻¹ PES with iron, 80 $\mu\text{E} \cdot \text{m}^{-2} \cdot \text{s}^{-1}$ white light and 14:10 h light:dark cycle. Diving PAM settings for the RLCs were adjusted for the lower light conditions in the laboratory: light curve intensity (LC-INT = 2), duration of each step (LC-WIDTH = 10 s) and activity light list for each step (0, 5, 18, 30, 42, 69, 97, 133 and 195 $\mu\text{mol} \cdot \text{m}^{-2} \cdot \text{s}^{-1}$). All individuals were flash-frozen in liquid nitrogen after 120 h. An additional 15 individuals were also flash-frozen at the beginning and another 15 at the end of the experiment for a transcriptomic baseline. Due to sporophyte growth problems in one of the NC populations and no sporophyte recruitment in one of the S populations, these two regions only had one replicate population. The 17°C treatment and the NC region at 24 h were removed from the data analysis as temperature fluctuations were recorded in the 17°C culture chamber, resulting in inconsistent ecophysiological responses and potentially compromising the data analysis and interpretation.

Statistical analyses of experimental data

In order to assess ecophysiological responses to temperature and nutrients in *M. pyrifera* from different regions, generalized linear models were used (GLMs; McCullagh & Nelder, 1989).

Experiment 1) - Adult blades: Four levels of the factor “Region” (N, NC, SC, and S), three levels of the factor “Temperature” (15, 20 and 24°C), two levels of the factor “Nutrients” (PES-enriched and non-enriched SW) and two levels of the factor “Depth” (surface and bottom) were used as fixed effects. The response variables were minimum saturating irradiance (E_k), maximum potential relative ETR ($r\text{ETR}_{\text{max}}$) and the photosynthetic rate in light-limited region of RLC (α), and the maximum quantum yield of PSII (F_v/F_m). All parameters were estimated from the rapid light curves (computed with rPackage phytotools (Silsbe & Sairah, 2015, CRAN repository), by fitting the model of Platt *et al* (1980). Analysis of variance (ANOVA) and post-hoc tests (Tukey Honest Significant differences (HSD)) were used to analyze the differences amongst treatments using R software (R Development Core Team, 2008). F_v/F_m and α were square root transformed to approximate residuals to a normal distribution. Since only a short acclimation period was possible, and to minimize any effects

of transportation on physiological responses, data from the RLCs were analyzed at the end point of the respective temperature treatments.

Experiment 2) - Entire individual vs removed blade: ANOVA and post-hoc tests (Tukey HSD) were used to analyze the difference between treatments using F_v/F_m as the variable for two levels of factor “Temperature” (16 and 24°C), two levels of the factor “Nutrients” (PES-enriched and non-enriched seawater) and three levels of factor “Tissue” (juvenile, juvenile blade and adult blade). F_v/F_m was square rooted transformed and the GLMs fitted using the Gaussian family (highest AIC) and resulting residuals were approximate to the normal distribution.

Experiment 3) - F1 generation juvenile sporophytes: Four levels of the factor “Region” (N, NC, SC and S), three levels of the factor “Temperature” (15, 19 and 21°C) and two levels of the factor “Nutrients” (PES-enriched and non-enriched SW) were used as fixed effects with the response variables α , Ek , ETR_{max} (estimated by the Diving PAM software Win-Control 3, Walz GmbH, Effeltrich, Germany) and F_v/F_m . GLMs were fitted using the Gaussian family distribution for all variables (selected by AIC comparison with the available distributions for R). The variable F_v/F_m was square root transformed and residuals were approximate to the normal distribution. Analysis of variance (ANOVA) and Tukey (HSD) were used to analyze the differences amongst treatments using R software (R Development Core Team, 2008). For the first and third experiments, we used populations within the same region as a replicate for that region.

Results

Common-garden experiment comparing adult blades (Experiment 1)

Our results showed that *Macrocystis pyrifera* blades from all regions performed well at 15°C and 20°C but were rapidly stressed at 24°C. At this temperature, more than 88 % of the blades had lower mean F_v/F_m values compared with the other treatments. At 24°C there was tissue degradation (*e.g.* necrotic tissue and loss of pigmentation) and mucilage production. Therefore, the experimental treatments at this temperature had to be terminated earlier while at the other temperatures the blades remained in culture in good condition. Rapid light curves (RLCs) parameters (α , Ek and $rETR_{max}$) and F_v/F_m measured at the end point of each temperature treatment confirmed that 24°C treatment rapidly stressed *M. pyrifera* blades (Fig. 3). Since no main effect or interactions involving nutrients were detected, non-enriched and PES-enriched treatments were combined for the plots in Figure 3.

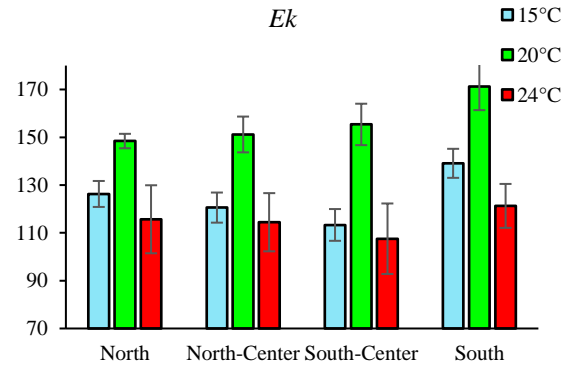
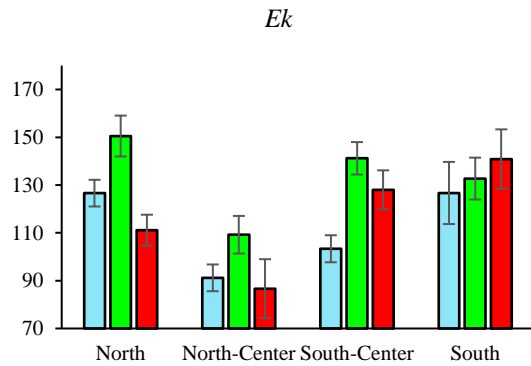
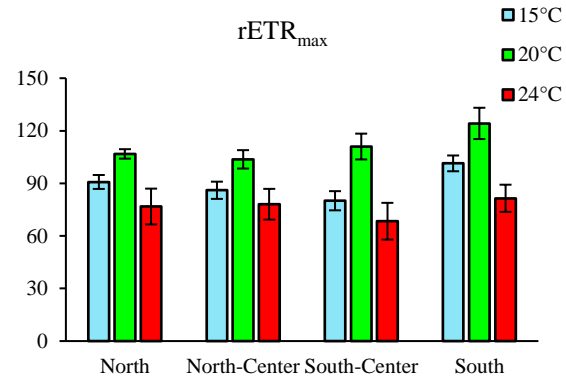
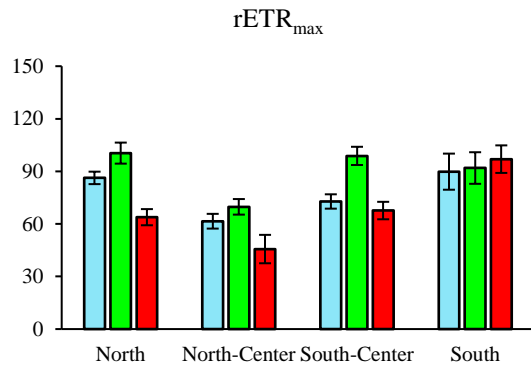
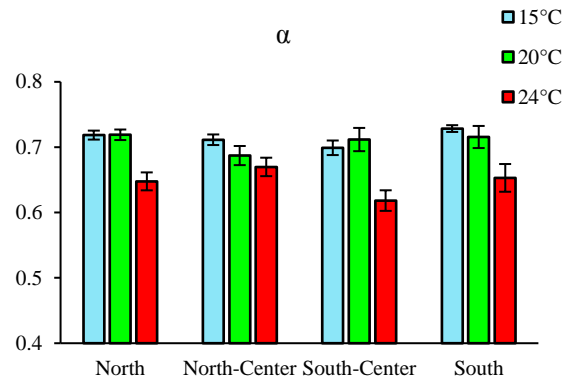
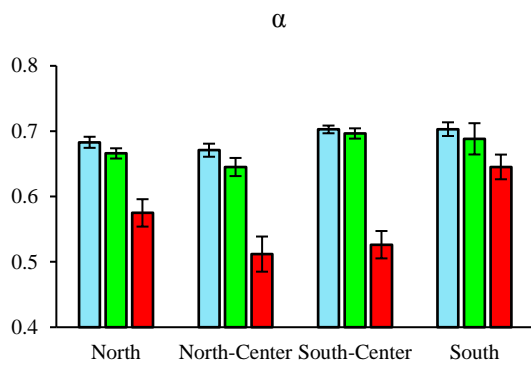
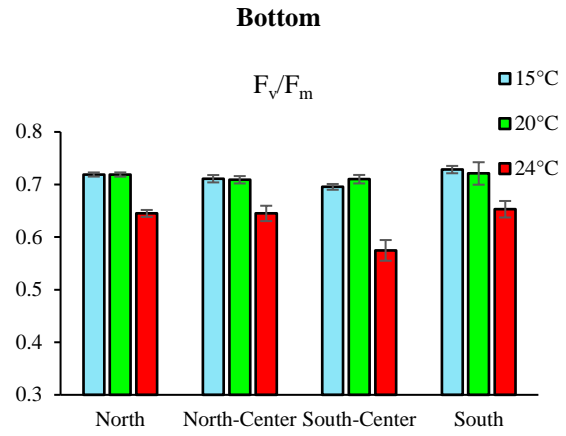
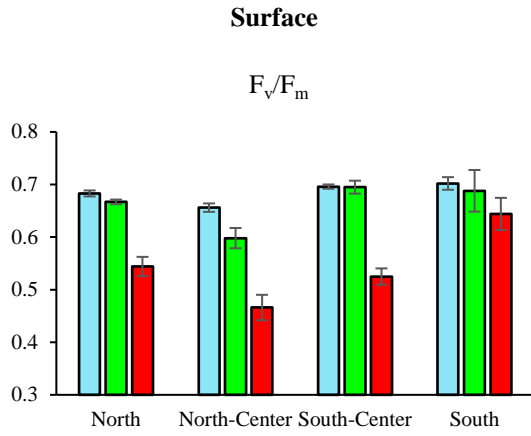


Figure 3: Maximum quantum yield of PSII (F_v/F_m), photosynthetic rate in light-limited region of RLC (α), relative maximum electron transport rate ($rETR_{max}$) and minimum saturating irradiance (E_k) mean values (\pm mean standard error) for 3 temperatures (15, 20, 24°C) and 4 regions (North, North-Center, South-Center and South) of adult blades over time. Different letters indicate significant differences among temperatures within each region and variable using Tukey HSD.

Maximum quantum efficiency of PSII (F_v/F_m)

Decreasing values of F_v/F_m can provide a rapid indication of stress affecting PS II in the dark-adapted state. With F_v/F_m as response variable, ANOVA indicated significant interactions due to Region x Temperature, Temperature x Depth and Region x Depth (Table 1).

The interaction between Region x Temperature revealed significant differences between regions in the response to thermal stress: In the N, NC, and SC regions, F_v/F_m was lower at 24°C than at either 20°C or 15°C (and attributable mainly to stress in surface blades), but in the S region significantly lower F_v/F_m was only detected between 24°C and 15°C ($p = 0.040$). The region differences were clear when responses at 24°C between regions at 24°C were considered; F_v/F_m was higher at 24°C in the S versus either SC or NC regions ($p = 9.5 \times 10^{-5}$ and 2.3×10^{-6} , respectively), but was marginally insignificant between S and N regions ($p = 0.066$).

Post-hoc tests (Tukey HSD) indicated that the interaction between Temperature x Depth (*i.e.*, surface and bottom blades) was due to greater resilience of F_v/F_m in bottom blades at 20°C and 24°C ($p = 0.001929$ and $p < 0.0001$, respectively), while in 15°C control conditions no differences in blade sampling depth were detected ($p > 0.25$).

Finally, the interaction between Region x Depth was due to significant contrasts involving surface blades between regions; more specifically F_v/F_m in NC surface blades was lower overall than in all other regions (NC < N, $p = 0.00136$; NC < SC, $p = 0.00027$; NC < S, $p = 8 \times 10^{-7}$). In addition, bottom blades had significantly greater F_v/F_m than surface blades in the N and NC regions, but not in the SC or S (Fig. 3).

Light-limited photosynthetic rates (α)

Analysis of α values revealed a significant interaction between Region x Temperature x Depth and post-hoc tests (Tukey HSD) highlighted that regional differences regarding the response to thermal stress (24°C) were due to significantly higher α values on the S region surface blades compared to NC and SC regions ($p = 7.19 \times 10^{-5}$ and $p = 2.82 \times 10^{-5}$, respectively) as other interactions were non-significant ($p > 0.275$). The response to thermal stress of the S region surface blades showed surprising stress tolerance, as all post-hoc tests between surface blades at 24°C and either 15 or 20°C temperatures were non-significant ($p > 0.742$), indicating that α was little affected over this temperature range. The same contrasts were significant for all other regions ($p \leq 0.00023$ in all cases). Also all regional comparisons between the 24°C treatments for the bottom blades were non-significant ($p \geq 0.698$). The effect of the 24°C surface blades on the interaction was also attested by the analysis of the α values between and within the 15°C control and 20°C that showed no significant differences between or within depths considering all possible regional combinations (total 120 combinations) with only one residual significant value ($p = 0.046$). Because both α and F_v/F_m represent aspects of photosynthetic efficiency (Kirk, 2011), the values reported were quite similar among temperatures within each region (Fig. 3).

Maximum electron transport rate ($rETR_{max}$)

Blades from all regions (exception for the S region surface blades) followed the same pattern in both depths as $rETR_{max}$ values were higher at 20°C, indicating increased photosynthetic performance when exposed to 20°C and photosynthetic inhibition by thermal stress when exposed to 24°C (Fig. 3). The post-hoc analysis of the interaction Region x Depth indicated that the significant regional differences were caused by significantly lower values in NC surface blades compared to other regions from the same depth (NC < N, $p < 0.001$; NC < SC, $p = 0.002$; NC < S, $p < 0.001$); no significant contrasts were found between regions when analyzing the blades collected from the bottom ($p > 0.257$). Treatment temperatures (e.g. 15, 20 and 24°C) differed significantly, with 18.5% and 29.5% higher $rETR_{max}$ values in blades at 20°C, when compared to 15°C and 24°C, respectively ($p < 0.001$) and 11% higher at 15°C

than at 24°C ($p < 0.001$). Again, the S region surface blades showed tolerance to thermal stress (*i.e.* 24°C) with no significant differences in $rETR_{\max}$ compared at 24°C compared with 20°C and 15°C (Fig. 3) ($p = 1.000$).

Minimum saturating irradiance (E_k)

The ANOVA analysis of E_k for adult blades showed a significant main effect for Temperature, and a significant interaction between Region x Depth (*i.e.*, blade type). The patterns of the response were similar to ETR_{\max} with a clear peak at 20°C for the majority of the regions (Fig. 3). The Region x Depth interaction (Table 1) resulted from significantly lower E_k values in NC surface blades (96.3) compared to the N (130.4407), SC (124.069) and S (134.25) regions (all $p \leq 0.001$) and no significant differences were found between surface blades for the other 3 regions ($p > 0.824$). Regional comparisons for E_k in bottom blades were non-significant ($p > 0.438$). At 20°C, E_k values were 19.6% and 20.8% higher overall compared to 15°C and 24°C, respectively ($p < 0.001$ for both comparisons), while no significant differences were found between 15°C and 24°C ($p = 0.783$). This result clearly demonstrates the thermal dependence of E_k with a peak near 20°C in N, NC, and SC regions. In contrast, E_k for S region surface blades was temperature independent across the thermal range tested, with no significant differences detected (all $p = 1.000$; Fig. 3). The thermal dependence of both E_k and ETR_{\max} is expected, since they are governed by the rate of enzymatic processes, and our results suggest that S region blades were better able to adjust photosynthetic rates across a broad temperature range between 15-24°C, in contrast to surface blades from more northerly regions.

The overall picture that emerged was that the NC region (Santa Barbara, Southern CA) was particularly sensitive to thermal effects on F_v/F_m , particular for surface blades. Overall, bottom blades showed greater resilience than surface blades. There was also a clear tendency in the S region towards thermal stress resilience, followed, surprisingly, by N regional populations (Santa Cruz, Central CA).

Table 1: Four-way ANOVA for the effects of Region, Temperature, Nutrients and Depth on the maximum quantum yield of PSII (F_v/F_m), photosynthetic rate in light-limited region of RLC (α), maximum electron transport rate (ETR_{max}) and minimum saturating irradiance (Ek) mean values of adult blades. Significant p-values are marked in bolt.

F_v/F_m					
Factor	df	SS	MS	F	p-value
Region	3	0.063	0.021	8.268	< 0.001
Temperature	2	0.488	0.244	96.204	< 0.001
Nutrients	1	0.002	0.002	0.646	0.422
Depth	1	0.138	0.138	54.239	< 0.001
Region:Temperature	6	0.044	0.007	2.867	0.010
Region:Nutrients	3	0.018	0.006	2.368	0.070
Region:Depth	3	0.072	0.024	9.524	< 0.001
Temperature:Nutrients	2	0.006	0.003	1.158	0.315
Temperature:Depth	2	0.031	0.015	6.058	0.003
Nutrients:Depth	1	0.001	0.001	0.366	0.545
Region:Temperature:Nutrients	6	0.022	0.004	1.459	0.191
Region:Temperature:Depth	6	0.020	0.003	1.331	0.242
Region:Nutrients:Depth	3	0.008	0.003	1.038	0.376
Temperature:Nutrients:Depth	2	0.006	0.003	1.095	0.336
Region:Temperature:Depth:Nutrients	6	0.018	0.003	1.174	0.319
α					
Factor	df	SS	MS	F	p-value
Region	3	0.016	0.005	4.265	0.010
Temperature	2	0.277	0.138	110.182	< 0.001
Nutrients	1	0.000	0.000	0.006	0.939
Depth	1	0.074	0.074	58.612	< 0.001
Region:Temperature	6	0.030	0.005	3.918	0.001
Region:Nutrients	3	0.002	0.001	0.545	0.652
Region:Depth	3	0.015	0.005	3.985	0.008
Temperature:Nutrients	2	0.005	0.003	2.056	0.130
Temperature:Depth	2	0.029	0.015	11.570	< 0.001
Nutrients:Depth	1	0.000	0.000	0.005	0.943
Region:Temperature:Nutrients	6	0.012	0.002	1.572	0.155
Region:Temperature:Depth	6	0.018	0.003	2.413	0.027
Region:Nutrients:Depth	3	0.002	0.001	0.504	0.680
Temperature:Nutrients:Depth	2	0.001	0.001	0.415	0.661
Region:Temperature:Depth:Nutrients	6	0.011	0.002	1.520	0.171

rETRmax

Factor	df	SS	MS	F	p-value
Region	3	17909	5970	9.516	< 0.001
Temperature	2	60023	30012	47.839	< 0.001
Nutrients	1	364	364	0.58	0.447
Depth	1	13760	13760	21.934	< 0.001
Region:Temperature	6	3278	546	0.871	0.516
Region:Nutrients	3	228	76	0.121	0.948
Region:Depth	3	8223	2741	4.369	0.005
Temperature:Nutrients	2	592	296	0.472	0.624
Temperature:Depth	2	1148	574	0.915	0.402
Nutrients:Depth	1	94	94	0.15	0.699
Region:Temperature:Nutrients	6	3712	619	0.986	0.435
Region:Temperature:Depth	6	3916	653	1.04	0.399
Region:Nutrients:Depth	3	3495	1165	1.857	0.137
Temperature:Nutrients:Depth	2	286	143	0.228	0.796
Region:Temperature:Depth:Nutrients	6	7123	1187	1.892	0.082

Ek

Factor	df	SS	MS	F	p-value
Region	3	26036	8679	7.816	< 0.001
Temperature	2	74820	37410	33.693	< 0.001
Nutrients	1	807	807	0.727	0.395
Depth	1	7284	7284	6.56	0.011
Region:Temperature	6	6562	1094	0.985	0.435
Region:Nutrients	3	551	184	0.165	0.920
Region:Depth	3	15432	5144	4.633	0.003
Temperature:Nutrients	2	264	132	0.119	0.888
Temperature:Depth	2	6577	3288	2.962	0.053
Nutrients:Depth	1	227	227	0.204	0.652
Region:Temperature:Nutrients	6	7125	1188	1.07	0.381
Region:Temperature:Depth	6	7887	1315	1.184	0.314
Region:Nutrients:Depth	3	7744	2581	2.325	0.075
Temperature:Nutrients:Depth	2	242	121	0.109	0.897
Region:Temperature:Depth:Nutrients	6	13871	2312	2.082	0.055

Oceanographic data

Short term climatology (2.5 months centered on the sampling day) showed a latitudinal gradient of temperature increase towards the south but with only small differences between the SC and NC regions, particularly during the days before the sampling day (vertical lines; Fig.4).

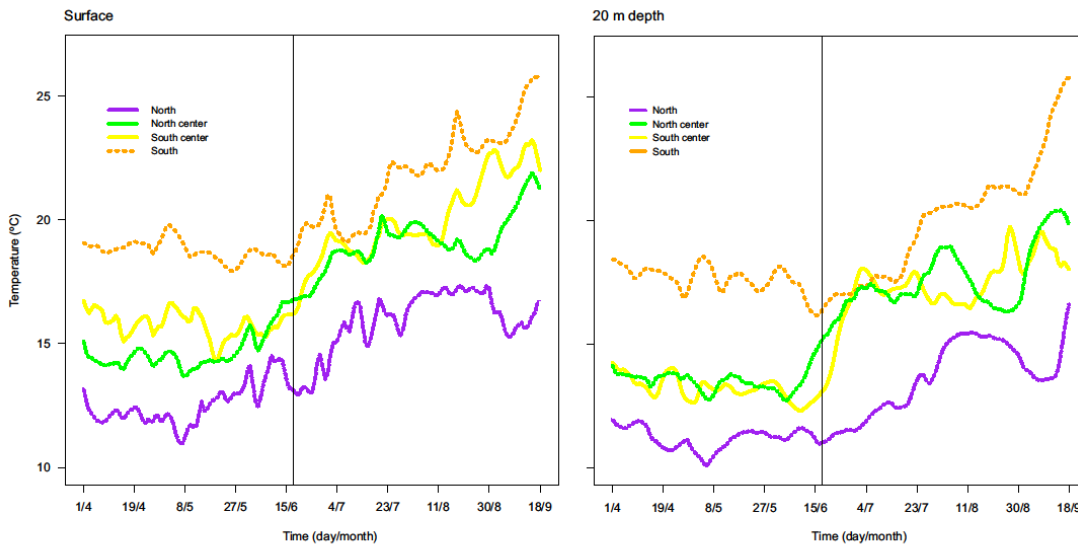
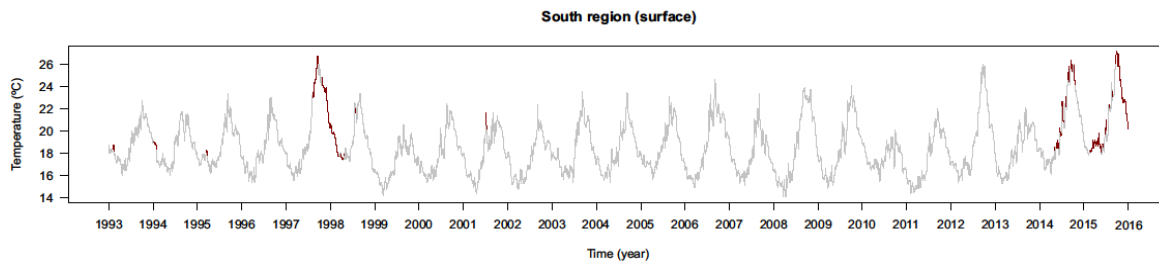


Figure 4: Daily mean seawater temperature (°C) on the 4 regions (North, North-Center, South-Center, South), at the surface (left) and 20m depth (right) centered on our sampling day (17/06/2017; vertical lines) using data collected from the Global Ocean Physics Reanalysis ECMWF ORAP5.0.

Previously to our sampling, the S region registered a continuous high temperature while the remaining regions presented a pattern of increasing temperatures. The NC region actually had higher temperatures than the SC region over several days prior to sampling, especially at 20m depth. Seawater (SW) temperatures at 20 m depth showed lower values when compared to the surface. On the sampling day, cooler 20 m SW had a mean difference to the warmer surface of between 2 and 3°C. During the months following the sampling, a persistent pattern of water temperature increase was predominant in which 25°C was reached in the S region by mid-September.

Temperature climatologies were compiled for the S region on the surface and bottom (20 m depth) over the last 22 years (Fig. 5)

a)



b)

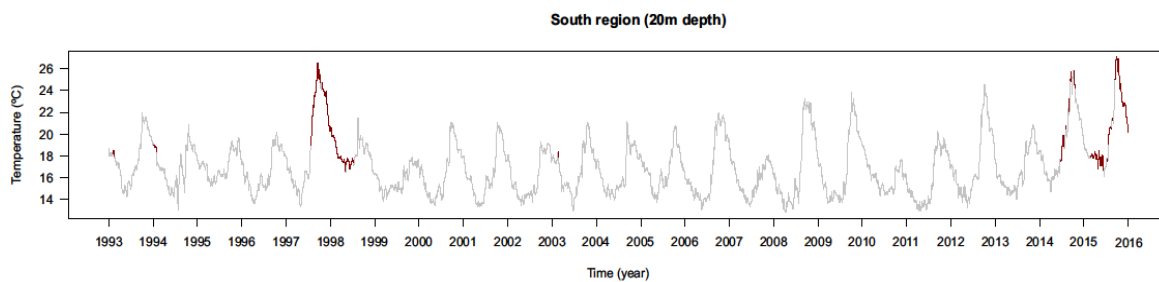


Figure 5: Climatologies of the South region surface (a) and 20m depth (b) over the past 22 years. Marine heat waves (MHWs) are marked in red (according to Hobday *et al.*, 2016).

Marine heat waves (an anomalously warm event lasting five or more days, with temperatures warmer than the 90th percentile based on a 30-year historical baseline period [Hobday *et al.*, 2016] greatly increased during the El Niño event the 1997-98, but also in 2014 and 2015 including during our sampling campaign (Table 4).

Table 2: Climatologies resume of the sampling sites (region) over the last 22 years for the seawater surface and 20m depth for the years with marine heat waves (MHW) and mean temperature (°C) during MHWs.

Region	Depth	Years with heat waves	Mean temperature during Heat wave (°C)
North	Surface	1993 1995 1997 1998 2005 2009 2014 2015	15.447±0.958
	20m depth	1993 1994 1995 1996 1997 1998 2003 2005 2006 2014 2015	14.329±1.984
North-center	Surface	1993 1994 1995 1996 1997 1998 2001 2005 2006 2009 2013 2014 2015	15.869±1.048
	20m depth	1993 1995 1996 1997 1998 2000 2005 2006 2009 2013 2014 2015	15.902±1.019
South-center	Surface	1995 1996 1997 1998 2005 2006 2010 2013 2014 2015	17.990±1.130
	20m depth	1993 1995 1996 1997 1998 2001 2003 2005 2006 2010 2014 2015	17.070±1.820
South	Surface	1993 1994 1995 1997 1998 2000 2001 2006 2014 2015	21.243±2.173
	20m depth	1993 1994 1997 1998 2003 2014 2015	20.185±2.463

All regions registered MHW during 2014-15 in both depths which suggests recent increase on the frequency of these extreme events.

Comparison of entire individuals vs excised blades (Experiment 2)

The photosynthetic response (F_v/F_m) over time for three different types of blades (entire juveniles, excised adults and juvenile blades) to thermal and nutrient stress is shown in (Fig. 6).

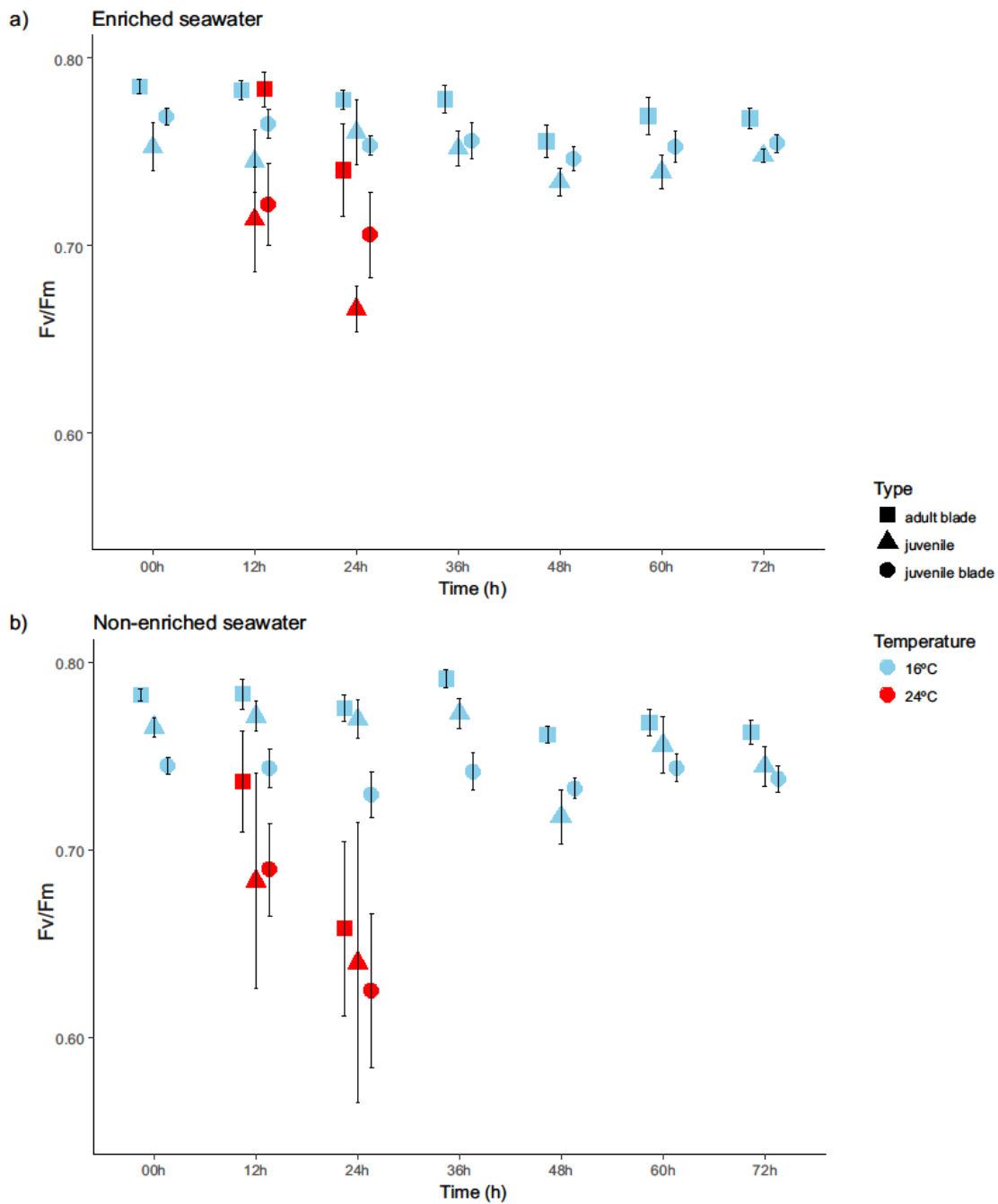


Figure 6: Maximum quantum yield of PSII (F_v/F_m) mean values (\pm mean standard error) for 2 temperatures (16 and 24°C) and 3 types (adult blade, juvenile blade and juvenile) on a) enriched seawater with PES (20 mL.L⁻¹) and b) non-enriched seawater, over time.

As in the previous experiment, blades and entire individuals at 16°C showed rather constant F_v/F_m over time while exposure to 24°C resulted in a rapid decrease, indicating a severe decline in PSII energy conversion efficiency. The ANOVA showed an interaction between Temperature x Nutrients and a significant main effect for the factor Tissue (Table 3). The post-hoc analysis (Tukey HSD) on the factor Tissue (*i.e.* juvenile, excised juvenile and adult blades) indicated no significant differences between the entire juvenile and the juvenile blade ($p = 0.995$), supporting the experiment design using excised blades in Experiment 1. Also in this analysis, significantly higher F_v/F_m values were found for adult blades (0.766) when compared with entire juvenile (0.737) and juvenile blade (0.736) ($p = 0.0000065$ and $p = 0.0000001$, respectively). Post-hoc tests (Tukey HSD) indicated that the interaction between Temperature x Nutrients was due to higher temperature as tissue at 24°C in enriched SW had significant lower F_v/F_m values than 16°C non-enriched and by nutrients when temperatures were at 24°C (see Annex II for mean values and *p-values*). The only exception was between 16°C enriched and 16°C non-enriched where differences in F_v/F_m were non-significant ($p = 0.848$). This experiment supports the use of excised blades as surrogate for entire individuals for *M. pyrifera* and that high temperature (24°C) in conjugation with low nutrients availability affects this species ecophysiological response, while having no effect at lower (non-stressful) temperatures (16°C), at least for 72h.

Table 3: Three-way ANOVA for the effects of Temperature, Nutrients and Type on the maximum quantum yield of PSII (F_v/F_m) mean values. Significant *p-values* are marked in bold.

Variable	Factor	df	SS	MS	F	p-value
F_v/F_m	Temperature	1	0.117	0.117	122.682	< 0.001
	Nutrients	1	0.010	0.010	10.795	0.001
	Tissue	2	0.037	0.018	19.293	< 0.001
	Temperature:Nutrients	1	0.022	0.022	22.603	< 0.001
	Temperature:Tissue	2	0.005	0.003	2.640	0.072
	Nutrients:Tissue	2	0.005	0.002	2.526	0.081
	Temperature:Nutrients: Tissue	2	0.001	0.001	0.532	0.588

Comparison of F1 generation juvenile sporophytes (Experiment 3)

F1 generation juvenile sporophytes of *M. pyrifera* grown *in vitro* and exposed to a thermal gradient over a 5-day simulated heat wave (15, 19 and 21°C) showed few region-specific patterns of stress induced by temperature increase, based on photosynthetic response parameters (F_v/F_m and the RLCs parameters α , ETR_{max} and Ek ; Fig. 7).

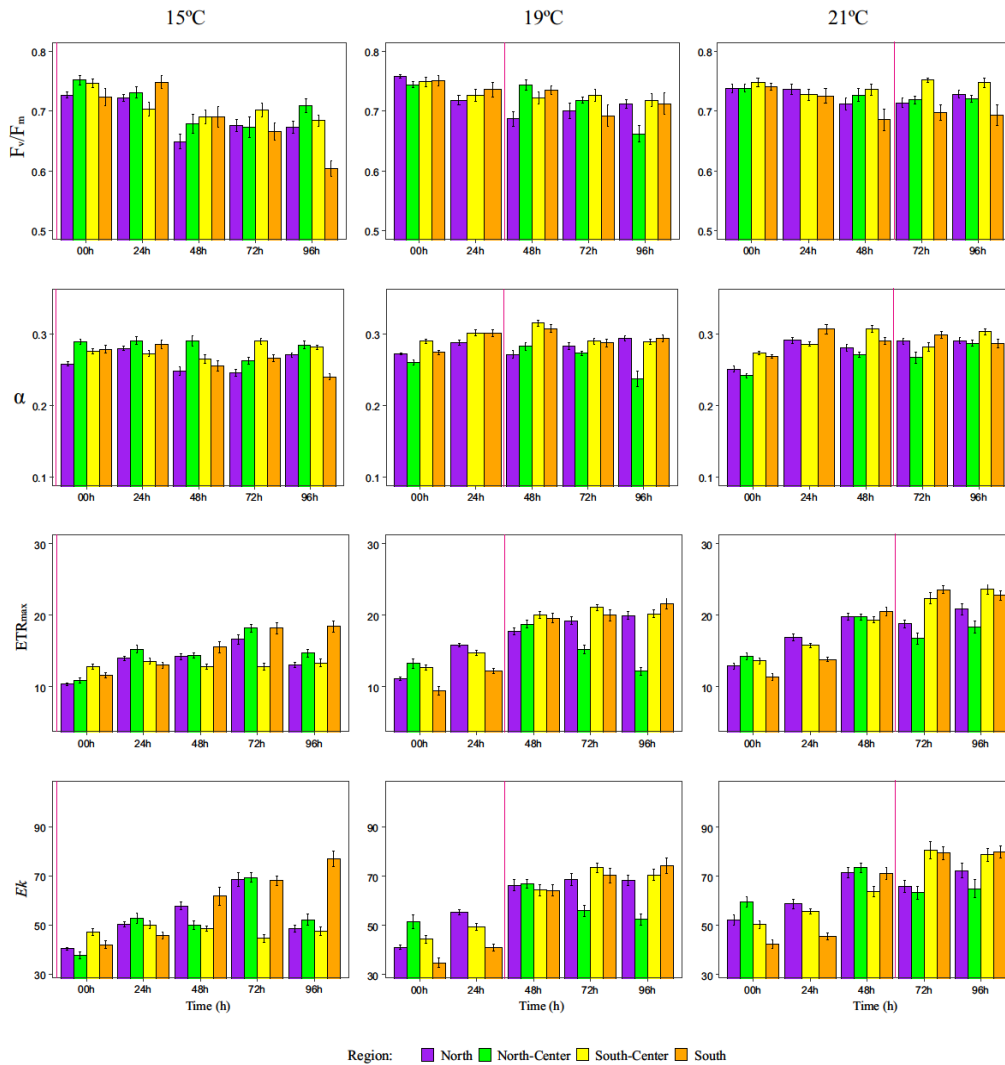


Figure 7: Maximum quantum yield of PSII (F_v/F_m), photosynthetic rate in light-limited region of RLC (α), maximum electron transport rate (ETR_{max}) and minimum saturating irradiance (Ek) mean values (\pm mean standard error) for 3 temperatures (15, 19, 21°C) and 4 regions (North, North-Center, South-Center and South) of F1 juvenile sporophytes over time. Vertical red line indicates the starting point for each temperature (time point when sporophytes were at that specific temperature for 24h). Different letters indicate significant differences among regions within each sampling time (00, 24, 48, 72 and 96h) for each temperature using Tukey HSD. North-Center region data at 24h on 19 and 21°C was removed due to values inconsistencies.

Maximum quantum efficiency of PSII (F_v/F_m)

Values for F_v/F_m in F1 juvenile sporophytes increased with increasing temperature as by the last sampling time (96 h) sporophytes at 21°C had higher F_v/F_m (0.725) when compared with the control (15°C) (0.671) although this increase was only significant for the SC region ($p = 0.006$) (Fig. 7). The interaction Region x Temperature (Table 4) was analyzed with post-hoc tests (Tukey HSD), which showed that within the same temperature, significant regional differences were only found at 21°C, in which the S region had significant lower F_v/F_m values (0.670) compared to N (0.721) and SC (0.749) regions ($p = 0.021$ and $p = 0.0000042$, respectively), but was not significantly different to the NC region (0.719; $p = 0.087$).

Light-limited photosynthetic rates (α)

The photosynthetic efficiency of juvenile F1 sporophytes as assessed from the initial slope of ETR vs. irradiance curves (α). With α as response variable, post-hoc tests on the interaction Region x Temperature revealed significant differences within temperature treatments, but in contrast to F_v/F_m no differences were found at 21°C (all $p > 0.252$), but only at 19°C and 15°C. At 15°C α values from the N region sporophytes (0.260) were significantly lower than either the NC (0.273) or SC (0.277) regions ($p = 0.00043$; $p = 0$, respectively), while SC had significantly greater α than the S region (0.266, $p = 0.0097456$). All regions showed a significant increase in α values at 21°C compared with controls at 15°C (S > 9%, $p = 0.001$; SC > 4.9%, $p = 0.011$; N 11.2%, $p = 0$) except for NC region (> 1.1%, $p = 0.999$).

Maximum electron transport rate ($rETR_{max}$)

An increase of ETR_{max} values with temperature and also time was observed during the experiment (Fig. 7). The analysis of the interaction Region x Temperature indicated a significant increase of regional differences with increasing temperature within the same region as ETR_{max} values were significantly higher at 21°C compared to the 15°C control (N > 33.4%; NC > 17.9%; SC 43%; S > 42%) ($p < 0.0000322$). All regional contrasts at 21°C

differ significantly ($p < 0.044$) except for S-SC regions ($p = 0.972$) but at 15°C significant differences were only found between NC region and the N and SC regions ($p = 0.034$ and 0.014, respectively). At 21°C the sporophytes from S and SC regions showed significant higher ETR_{max} (24.01 and 22.96, respectively) compared with NC and S regions (17.55 and 19.79, respectively) ($p < 0.004$).

Minimum saturating irradiance (Ek)

F1 sporophyte Ek values followed a similar pattern to ETR_{max} as the Region x Temperature interaction pointed again to significant contrasts at higher temperatures, with tissue within each region at 21°C showing Ek mean values 31% greater overall than 15°C control (all $p \leq 0.002$). Regional differences were also higher at 21°C as northern regions showed significantly lower Ek values (N = 68.8 and NC = 63.88) compared with the southern regions (SC = 79.49 and S = 82.40; all $p \leq 0.001$). No significant differences were found within the groups (N-NC, $p = 0.836$ and SC-S, $p = 0.999$). At 15°C, a strong reduction in Ek was observed at 96 h, but interestingly S region sporophytes Ek values continued to increase, being at least 32.33% higher than the other regions.

Table 4: Two-way ANOVA for the effects of Region and Temperature on the maximum quantum yield of PSII (F_v/F_m), photosynthetic rate in light-limited region of RLC (α), maximum electron transport rate (ETR_{max}) and minimum saturating irradiance (Ek) mean values of F1 juvenile sporophytes. Significant p-values are marked in bolt.

Variable	Factor	df	SS	MS	F	p-value
F_v/F_m	Region	3	0.033	0.011	9.577	< 0.001
	Temperature	2	0.009	0.004	3.771	0.023
	Region:Temperature	6	0.024	0.004	3.502	0.002
α	Region	3	0.049	0.016	28.820	< 0.001
	Temperature	2	0.087	0.043	76.160	< 0.001
	Region:Temperature	6	0.037	0.006	10.730	< 0.001
ETR_{max}	Region	3	426	142	15.650	< 0.001
	Temperature	2	12133	6066	668.050	< 0.001
	Region:Temperature	6	1232	205	22.610	< 0.001
Ek	Region	3	2460	820	5.216	0.0014
	Temperature	2	107682	53841	342.405	< 0.001
	Region:Temperature	6	11060	1843	11.722	< 0.001

Discussion

Regional differences and potential for local adaptation

The results of our common garden experiment clearly showed that populations of *M. pyrifera* at the southernmost limit of the species distribution in the northern hemisphere displayed greater thermal tolerance in their photosynthetic physiology. This suggests an important effect of the highly selective thermal conditions of the southernmost kelp habitat. This better performance of South (S) region populations was more clearly seen in the blades collected at the water surface, which were able to maintain similar maximum electron transport rate (ETR_{max}) values at temperatures between 15-24°C, and in contrast to more northerly populations. The rather clear patterns of thermal tolerance in the S region surface blades was much less evident in blades from deeper waters (bottom blades), the responses of which were rather similar between regions.

Given the constraints of the experiment, in particular the short pre-acclimation period, these differences can either be attributed to intrinsic (*i.e.*, genetically-determined) variation, or to plasticity induced by an environmental history of higher temperatures in southern surface waters (up to 20°C; Fig. 4). Wave height increase might also have impacted the kelp forests of the south region as the hurricane Blanca, the second of the season, moved near the populations two weeks before our sampling campaign. In the field, the southern population (Bahia Tortugas) had a lower canopy cover (sparse distribution of individuals) and showed signs of greater stress (lower pigmentation, damaged tissue) compared with populations in more northern regions. The differences observed between the S and SC regions are all the more intriguing given that genetic analysis with microsatellites (neutral genetic markers) indicated that these two regions form a single genetic cluster (Johansson *et al.*, 2015). We conclude that, while the results are consistent with local genetic adaptation, this hypothesis will require further analysis and confirmation via the transcriptomes extracted from the individuals across the experiments, particularly those derived from the F1 generation cultured *in vitro* from parental reproductive material.

Individuals from the North-Center (NC) region showed a consistently poor photosynthetic response to thermal and nutrients stressors compared with other regions using both acclimated field-collected blades (Experiment 1) and in vitro F1 sporophytes (Experiment 3). As F1 juveniles were grown in common-garden laboratory conditions, the effects of environmental history can safely be excluded (assuming no or limited carry-over across generations and life-history phases). It can therefore be concluded that the NC populations are intrinsically less able to cope with stress conditions due to genetic factors. A possible reason might be elevated levels of self-fertilization and inbreeding in NC populations. Previous studies in the Santa Barbara bay area showed that self-fertilization greatly reduced *M. pyrifera* fitness (survival to adulthood, zygote production, development of reproductive structures and fecundity) (Raimondi *et al.*, 2004). The study of Johansson *et al.*, (2013) reported a high self-fertilization rate (32-44%) and strong correlation between inbreeding depression and mortality. Although this hypothesis requires an objective study and analysis at the regional level, our results suggest that reproductive strategies and constraints such as inbreeding and self-fertilization may be important factors regulating regional differences underlying local population dynamics.

The North (N) and South-Center (SC) regions adult blades showed similar intermediate photosynthetic responses to stress conditions with no significant differences between them (Table 1, Fig. 3). N region blades from both depths were in very good conditions, with almost no tissue damage or mucilage production and good pigmentation which might reflect local field conditions prior to our experiment as SW temperatures were below 15°C in the area. The good ecophysiological conditions might have contributed to the increase of photosynthetic efficiency of surface blades (α) compared to the other regions but F_v/F_m and ETR_{max} were lower than the S region, suggesting greater stress on the photosynthetic apparatus. The N region kelp forests are located ~ 300 km north of the phylogeographical break of Point Sal (Johansson *et al.*, 2015), 50Km north of the biogeographic break of Point Conception, a boundary characterized by a 5°C north-south temperature gradient caused by the interaction of the cold California current with the California Eddy (Burton, 1998; Eberl *et al.*, 2013). The mean surface temperature during a MHW over the last 22 years is 15.447°C \pm 0.958 in this region. This suggests that these populations are not exposed to the same level of thermal/nutrient stress experienced by the southern regions, and may putatively be less

able to cope with such stresses. Our regional analysis did not, however, show a clear latitudinal gradient of ecophysiological response of the giant kelp to thermal and nutrient stresses, which could be due to several factors: heterogeneity of oceanographic/atmospheric processes (Pacific decadal oscillation (PDO), El Niño and La Niña, California current, California Eddy, upwelling areas, internal waves) (Burton, 1998; Fram *et al.*, 2008; Ladah *et al.*, 2012 ; Newman *et al.*, 2016; Jacox *et al.*, 2016) , or, as suggested by other authors, or by more local processes that interact at a smaller (population) scales such as competition, dispersal and reproduction, wave exposure, dispersal, forest depth and density (Dayton, 1999; Edwards, 2004; Edwards & Hernández-Carmona, 2005; Cavanaugh *et al.*, 2011; Cavanaugh *et al.*, 2013; Johansson *et al.*, 2015). Thus, in order to understand and predict possible implications of climate change on *M. pyrifera* forests on a regional level, further studies should focus on understanding the fundamental processes that act locally and how they interact with larger scale processes.

Thermal limits

This study showed that at 24°C adult blades from almost all regions of *Macrocystis pyrifera* studied showed a strong decline in ecophysiological responses. However, the exception was surface blades from the southernmost region, which did not follow general trends with respect to temperature-sensitive photosynthetic parameters E_k and $rETR_{max}$. While F_v/F_m and the slope of electron transport rate with increasing irradiance (α) showed a similar pattern of photosynthetic rate decrease with increasing temperature, $rETR_{max}$ and E_k increased from 15 to 20 °C followed by a decrease at 24 °C. This temperature trend is typical of rate-limited enzymatic processes in, e.g., Calvin cycle enzymes such as RuBisCO (Kirk, 2011). When temperature was increased to 24°C the thermal optimum for photosynthesis was exceeded and the entire network was affected. The exception to this pattern was the S region surface blades in which ETR_{max} and E_k did not differ between 15 and 24°C, suggesting either pre-acclimation or adaptation to local conditions with warmer SW temperatures.

It appears that the thermal limits of photosynthetic performance were not exceeded in Experiment 3 using F1 juvenile sporophytes, in which 21°C was the maximum exposure temperature. It is also possible that the use of gradual thermal ramping may have alleviated

the effects of thermal stress in this experiment (2°C increments per 24 h up to the target temperature), compared with the direct shock used in the 1st and 2nd experiments. As a result, F1 sporophytes showed increasing ETR_{max} and Ek with increasing temperature, particularly in the SC and S regions. We decided on this approach based on the results and observations of the last two experiments, as well as published experiments showing that juveniles under stress conditions survive less well than adults (Dean & Jacobsen, 1984), the small size and thickness of the F1 sporophytes and the necessity to avoid sampling necrotic tissue that would jeopardize further transcriptomic analysis. Although F1 sporophytes were not subjected to substantial disturbance to the photosynthetic apparatus, e.g., decline in F_v/F_m at higher temperatures, it was nevertheless significant that differences in thermally-sensitive enzymatic processes (Ek and $rETR_{max}$) could be distinguished between S/SC (higher performance) and N/NC (lower performance) regions. However, further experiments will be required to explore the effects of higher temperatures on the upper thermal limits for photosynthetic performance and other (e.g., growth) responses.

Climatology data for the months prior to our sampling showed that the central regions (NC and SC) shared similar thermal regimes, while the N region dominated by the cold California current had lower temperatures and S region was already experiencing high SW temperatures (Fig. 4). The low canopy cover of the southernmost populations may have reflected the prevailing thermal conditions, in addition to which local populations composed of juveniles and small adult sporophytes were still regrowing after they disappeared during the summer of 2014 (personal communication by the local fisherman). This information is supported by the 22 y climatology data of the S region (Fig. 5) which showed a great increase in MHW frequency in the summer of 2014 and spring of 2015. Selection pressure for acclimation/survival of individuals more adapted to higher temperatures prior to sampling is therefore clearly possible. Our data also showed an unprecedented increase frequency, duration and intensity of MHWs that for the first time in 22 years occurred for two consecutive years (2014-15) (see also Table 2); phenomena reported on the study area by several other authors (Bond *et al.*, 2015 ; Jacox *et al.*, 2016; Levine & Mcphaden, 2016; Reed *et al.*, 2016; Cohen *et al.*, 2017). While temperature itself can directly impact the vital processes of the giant kelp, including photosynthesis, SW temperature increase is inversely related to nutrients concentration and indeed has been widely used as a proxy for nutrient

concentration (Kamykowsk, 1977; Dugdale *et al.*, 1989; Zimmerman & Kremer, 1984; Switzer *et al.*, 2003; Reed *et al.*, 2016).

Nutrient effects

The nutrient treatments tested in Experiment 1 (enriched and non-enriched SW with PES) did not showed clear effects on the photosynthesis rates of the adult blades. This lack of effect was evident as the RLCs parameters and F_v/F_m showed no significance on the Nutrients and no interaction was found with the other factors (Table 1). A likely reason is that even though *M. pyrifera* adult sporophyte nutrient and photosynthate storage capabilities are considered to be small (only 2-3 weeks) (Gerard, 1982) the short duration of the experiment (max. 72 h) did not result in significant depletion of reserves. Another reason might be that the nutrient concentration on the SW used on our experiment was already above non-limiting concentrations, even though it was collected from stationary reservoirs where the SW is stored for several days at relatively high temperatures. The analysis of the water sampled during the experiment 1 from each treatment was not available by the writing of this thesis but will certainly be used to clarify our results in future publications. On the other hand, significant nutrients effects and interaction with temperature were observed in experiment 2 (Table 3). Our results showed that at higher temperatures (*i.e.* 24°C) photosynthetic rates (F_v/F_m) were significantly lower in the non-enriched treatments compared to the PES-enriched treatments, although no significant differences were found at 16°C control. This illustrates a positive relationship between nutrient availability and thermal stress tolerance to warmer temperatures. Our results are in agreement with a recent study on another Kelp, *Saccharina japonica*, where nutrient availability significantly increased growth rates and survival of juveniles and adults (blade discs) at warmer temperatures (Gao *et al.*, 2017). In two separate field experiments using nutrient fertilization, *M. pyrifera* responded positively to thermal stress (warm seawater periods) when nutrient availability was increased, resulting in reduction of adult canopy loss (North, 1983) and increase of juvenile survival (Hernandez-Carmona *et al.*, 2001). Thus our further research will also include a non-enriched treatment (using controlled artificial SW) in order to understand the possible synergistic effect of nutrients at warm SW temperature on the F1 juvenile sporophytes.

Depth effects

Consistent differences in the photosynthetic rates between surface and bottom blades were found, with surface blades showing a lower mean F_v/F_m and RLC parameters (α , $rETR_{max}$ and Ek) but also higher variance within these values, especially at 24 °C. Previous studies have found that the maximum photosynthetic and ETR rates of *M. pyrifera* blades decreased with depth and were mainly controlled by the vertical distribution of PAR in the water column (Colombo-Pallotta *et al.*, 2006). In that study, surface blades were found to be adapted for high photosynthetic production with high values of F_v/F_m and $rETR$ and protected from the high light intensity by UV-absorbing compounds and protective carotenoids while bottom blades had lower photosynthetic rates and were responsible for the nutrient uptake. This makes sense as an adaptation to the local environmental conditions in the Baja California warmer months: a stratified water column with an oligotrophic warm surface layer that is breached by deep cold, nutrient rich waters pulsed by upwelling and internal waves events (Ladah, 2003; Ladah *et al.*, 2012; Rodriguez *et al.*, 2016). In another study, old surface blades were found to have lower F_v/F_m values and higher variability compared to bottom blades but also strong diurnal variability photosynthetic performance (Edwards & Kim, 2010). During our experiment, surface blades from all regions also showed lower F_v/F_m values, lower pigmentation and were visibly more damaged than bottom blades. It is then safe to assume that the continuous exposure to UV, wave motion, higher temperatures and photosynthesis workload on surface blades resulted in higher cellular and external damage. The exposure to the experimental temperatures (24 °C) above the algae thermal optimum resulted in more rapid degradation of the surface blades. On the other hand bottom blades were in much better physiological condition and showed higher stability between regions for all RLCs parameters compared to the surface blades, a pattern also reported previously for *M. pyrifera* (Edwards & Kim, 2010).

Conclusions

Our findings suggest that populations of *M. pyrifera* from the southernmost region of the species distribution in the northern hemisphere, exhibit resilience to warmer ocean conditions compared to cooler, more northern regions. At the southern limit, higher photosynthetic rates under thermal stress were observed in field sampled adult blades acclimated and tested under common garden conditions. Importantly, with respect to mainly enzyme-limited photosynthetic processes ($rETR_{max}$, Ek), greater tolerance was seen *in vitro* F1 juveniles from the S and SC regions, suggesting that populations in these regions are locally adapted to the prevailing warmer ocean conditions. Despite the greater resilience to thermal stress, observed increasing frequency and intensity of MHWs and other disturbances such as hurricanes might result in a cumulative effect on the *M. pyrifera* forests, reducing the overall resilience of the ecosystem (Wernberg *et al.*, 2010).

We also observed a generally poor photosynthetic response to thermal stress in the NC region, which also carried over to the F1 generation. Climatological data showed a thermal regime in the NC region around Santa Barbara to be at least as warm as the SC area of Baja California. Therefore our experimental observations suggest some underlying genetic basis leading to reduced fitness (e.g., possible inbreeding; Raimondi *et al.*, 2004) in this region, which forms a distinct genetic group (Johansson *et al.*, 2015).

Our experiments also demonstrated that thermal stress tolerance of *M. pyrifera* might be enhanced by nutrient availability and highlights the need for future studies on this subject. Finally, the use of excised blades as a valid surrogate for entire individuals was verified for *M. pyrifera* juveniles, at least for short experimental periods (24-72h). Our further research will focus the analysis of the transcriptomes extracted from the adult blades and F1 juveniles in order to evaluate putative regional local adaptation and assess the synergy of nutrients and temperature stress on F1 sporophytes.

References

Adey, W. H., & Steneck, R. S. (2001). Thermogeography over time creates biogeographic regions: A temperature/space/time-integrated model and an abundance-weighted test for benthic marine algae. *Journal of Phycology*, 37(5), 677–698. <http://doi.org/10.1046/j.1529-8817.2001.00176.x>

Alberto, F., Raimondi, P. T., Reed, D. C., Coelho, N. C., Leblois, R., Whitmer, A., & Serrão, E. A. (2010). Habitat continuity and geographic distance predict population genetic differentiation in giant kelp. *Ecology*, 91(1), 49–56.

Alberto, F., Raimondi, P. T., Reed, D. C., Watson, J. R., Siegel, D. a, Mitarai, S., ... Serrão, E. a. (2011). Isolation by oceanographic distance explains genetic structure for *Macrocystis pyrifera* in the Santa Barbara Channel. *Molecular Ecology*, 20(12), 2543–54. <http://doi.org/10.1111/j.1365-294X.2011.05117.x>

Anderson, R. A. (2005). *Algal Culturing Techniques, 1st Edition*. Elsevier Academic Press *Phycological Society of America* (Vol. 53). <http://doi.org/10.1017/CBO9781107415324.004>

Assis, J., Coelho, N. C., Lamy, T., Valero, M., Alberto, F., & Serrão, E. Á. (2016). Deep reefs are climatic refugia for genetic diversity of marine forests. *Journal of Biogeography*, 43(4), 833–844. <http://doi.org/10.1111/jbi.12677>

Baker, N. R. (1991). A possible role for photosystem {II} in environmental perturbations of photosynthesis. *Physiologia Plantarum*, 81(4), 563–570. <http://doi.org/10.1111/j.1399-3054.1991.tb05101.x>

Balmaseda, M. A., Mogensen, K., & Weaver, A. T. (2013). Evaluation of the ECMWF ocean reanalysis system ORAS4. *Quarterly Journal of the Royal Meteorological Society*, 139(674), 1132–1161. <http://doi.org/10.1002/qj.2063>

Beer, S., Björk, M., & Beardall, J. (2014). *Photosynthesis in the marine environment*. Wiley Blackwell (Vol. 1). <http://doi.org/10.1017/CBO9781107415324.004>

Beer, S., & Koch, E. (1996). Photosynthesis of marine macroalgae and seagrasses in globally changing CO₂ environments. *Marine Ecology Progress Series*, 141(1–3), 199–204. <http://doi.org/10.3354/meps141199>

Beer, S., Vilenkin, B., Weil, A., Veste, M., Susel, L., & Eshel, A. (1998). Measuring photosynthetic rates in seagrasses by pulse amplitude modulated (PAM) fluorometry. *Marine Ecology Progress Series*, 174, 293–300. <http://doi.org/10.3354/meps174293>

Bell, T. W., Cavanaugh, K. C., Reed, D. C., & Siegel, D. A. (2015). Geographical variability

in the controls of giant kelp biomass dynamics. *Journal of Biogeography*, 42(10), 2010–2021. <http://doi.org/10.1111/jbi.12550>

Bond, N. A., Cronin, M. F., Freeland, H., & Mantua, N. (2015). Causes and impacts of the 2014 warm anomaly in the NE Pacific. *Geophysical Research Letters*, 42(9), 3414–3420. <http://doi.org/10.1002/2015GL063306>

Burton, S. R. (1998). Intraspecific Phylogeography Across the Point Conception Biogeographic Boundary. *Evolution*, 52(3), 734–745. <http://doi.org/10.2307/2411268>

Byrnes, J. E., Reed, D. C., Cardinale, B. J., Cavanaugh, K. C., Holbrook, S. J., & Schmitt, R. J. (2011). Climate-driven increases in storm frequency simplify kelp forest food webs. *Global Change Biology*, 17(8), 2513–2524. <http://doi.org/10.1111/j.1365-2486.2011.02409.x>

Caputi, N., Feng, M., Pearce, A., Benthuyesen, J., Denham, A., Hetzel, Y., ... Chandrapavan, A. (2015). *Management implications of climate change effect on fisheries in Western Australia. Part 1. Environmental change and risk assessment*. Retrieved from http://www.fish.wa.gov.au/Documents/research_reports/frr260.pdf

Cavanaugh, K. C., Kendall, B. E., Siegel, D. A., Reed, D. C., Alberto, F., & Assis, J. (2013). Synchrony in dynamics of California giant kelp forests is driven by a combination of local recruitment and regional environmental controls. *Ecology*, 94(2), 1–33. <http://doi.org/10.1890/12-0268.1>

Cavanaugh, K. C., Siegel, D. A., Reed, D. C., & Dennison, P. E. (2011). Environmental controls of giant-kelp biomass in the Santa Barbara Channel, California. *Marine Ecology Progress Series*, 429, 1–17. <http://doi.org/10.3354/meps09141>

Cohen, J., Pfeiffer, K., & Francis, J. (2017). Winter 2015/16: A turning point in ENSO-based seasonal forecasts. *Oceanography*, 30(1), 0–9. <http://doi.org/https://doi.org/10.5670/oceanog.2017.115>:

Colombo-Pallotta, M. F., García-Mendoza, E., & Ladah, L. B. (2006). Photosynthetic Performance, Light Absorption, and Pigment Composition of *Macrocystis Pyrifera* (Laminariales, Phaeophyceae) Blades From Different Depths. *Journal of Phycology*, 42(6), 1225–1234. <http://doi.org/10.1111/j.1529-8817.2006.00287.x>

Crispo, E., Dibattista, J. D., Correa, C. C., Thibert-Plante, X., McKellar, A. E., Schwartz, A. K., ... De León, L. F. (2010). The evolution of phenotypic plasticity in response to anthropogenic disturbance. *Evolutionary Ecology Research*, 12(1), 47–66.

Daniel, R. M., Dines, M., & Petach, H. H. (1996). The denaturation and degradation of stable enzymes at high temperatures. *Biochemical Journal*, 11, 1–11.

Davison, I. R. (1991). Environmental effects on algal photosynthesis: temperature. *Journal of Phycology*, 27, 2–8.

Dayton, P. K. T. M. J. E. B. P. R. L. K. (1999). Temporal and spatial scales of kelp demography: the role of oceanographic climate. *Ecological Monographs*, 69(2), 219–250. [http://doi.org/10.1890/0012-9615\(1999\)069\[0219:TASSOK\]2.0.CO;2](http://doi.org/10.1890/0012-9615(1999)069[0219:TASSOK]2.0.CO;2)

Dean, T. A., & Jacobsen, F. R. (1984). Growth of juvenile *Macrocystis pyrifera* (Laminariales) in relation to environmental factors. *Marine Biology*, 83, 301–311.

Dean, T. A., Schroeter, S. C., & Dixon, J. D. (1984). Effects of grazing by two species of sea urchins (*Strongylocentrotus franciscanus* and *Lytechinus anamesus*) on recruitment and survival of two species of kelp (*Macrocystis pyrifera* and *Pterygophora californica*). *Marine Biology*, 78(3), 301–313. <http://doi.org/10.1007/BF00393016>

Deyseher, L. E., & Dean, T. A. (1986). Interactive effects of light and temperature on sporophyte production in the giant kelp *Macrocystis pyrifera*. *Marine Biodiversity*, 93, 17–20.

Dugdale R, C., Morel, A., Bricaud, A., & Wilkerson, P. (1989). Modeling New Production in Upwelling Centers: A Case Study of Modeling New Production From Remotely Sensed Temperature and Color. *Journal of Geophysical Research*, 94(C12), 18,119-18,132. <http://doi.org/10.1029/JC094iC12p18119>

Eberl, R., Mateos, M., Grosberg, R. K., Santamaria, C. A., & Hurtado, L. A. (2013). Phylogeography of the supralittoral isopod *Ligia occidentalis* around the Point Conception marine biogeographical boundary. *Journal of Biogeography*, 40, 2361–2372. <http://doi.org/10.1111/jbi.12168>

Edwards, M. S. (2004). Estimating scale-dependency in disturbance impacts: El Niños and giant kelp forests in the northeast Pacific. *Oecologia*, 138(3), 436–447. <http://doi.org/10.1007/s00442-003-1452-8>

Edwards, M. S., & Hernández-Carmona, G. (2005). Delayed recovery of giant kelp near its southern range limit in the North Pacific following El Niño. *Marine Biology*, 147(1), 273–279. <http://doi.org/10.1007/s00227-004-1548-7>

Edwards, M. S., & Kim, K. Y. (2010). Diurnal variation in relative photosynthetic performance in giant kelp *Macrocystis pyrifera* (Phaeophyceae, Laminariales) at different depths as estimated using PAM fluorometry. *Aquatic Botany*, 92(2), 119–128. <http://doi.org/10.1016/j.aquabot.2009.10.017>

Fram, J. P., Stewart, H. L., Brzezinski, M. a., Gaylord, B., Reed, D. C., Williams, S. L., &

MacIntyre, S. (2008). Physical pathways and utilization of nitrate supply to the giant kelp, *Macrocystis pyrifera*. *Limnology and Oceanography*, 53(4), 1589–1603. <http://doi.org/10.4319/lo.2008.53.4.1589>

Gao, X., Endo, H., Nagaki, M., & Agatsuma, Y. (2017). Interactive effects of nutrient availability and temperature on growth and survival of different size classes of *Saccharina japonica* (Laminariales, Phaeophyceae). *Phycologia*, 56(January), 253–260. <http://doi.org/10.2216/16-91.1>

Garrabou, J., Coma, R., Bensoussan, N., Bally, M., Chevaldonné, P., Cigliano, M., ... Cerrano, C. (2009). Mass mortality in Northwestern Mediterranean rocky benthic communities: Effects of the 2003 heat wave. *Global Change Biology*, 15(5), 1090–1103. <http://doi.org/10.1111/j.1365-2486.2008.01823.x>

Gerard, V. A. (1982). Growth and utilization of internal nitrogen reserves by the giant kelp *Macrocystis pyrifera* in a low-nitrogen environment. *Marine Biology*, 66(1), 27–35. <http://doi.org/10.1007/BF00397251>

Graham, M. H. (2004). Effects of Local Deforestation on the Diversity and Structure of Southern California Giant Kelp Forest Food Webs. *Ecosystems*, 7(4), 341–357. <http://doi.org/10.1007/s10021-003-0245-6>

Graham, M. H., & Halpern, B. S. (2008). Diversity and Dynamics of Californian Subtidal Kelp Forests Chapter. In *Food Webs and the Dynamics of Marine Reefs* (Vol. Chapter 9«, pp. 1–26).

Graham, M. H., Vásquez, J. A., & Buschmann, A. H. (2007). Global Ecology of the Giant Kelp *Macrocystis*: from Ecotypes to Ecosystems. *Oceanography and Marine Biology*, 45, 39–88.

Halpern, B. S., Selkoe, K. A., Micheli, F., & Kappel, C. V. (2007). Evaluating and ranking the vulnerability of global marine ecosystems to anthropogenic threats. *Conservation Biology*, 21(5), 1301–1315. <http://doi.org/10.1111/j.1523-1739.2007.00752.x>

Hawkins, S. J., Southward, A. J., & Genner, M. J. (2003). Detection of environmental change in a marine ecosystem - evidence from the western English Channel. *Science of the Total Environment*, 310(1–3), 245–256. [http://doi.org/10.1016/S0048-9697\(02\)00645-9](http://doi.org/10.1016/S0048-9697(02)00645-9)

Henkel, S. K., & Hofmann, G. E. (2008). Thermal ecophysiology of gametophytes cultured from invasive *Undaria pinnatifida* (Harvey) Suringar in coastal California harbors. *Journal of Experimental Marine Biology and Ecology*, 367(2), 164–173. <http://doi.org/10.1016/j.jembe.2008.09.010>

Hernandez-Carmona, G., Robledo, D., & Serviere-Zaragoza, E. (2001). Effect of Nutrient Availability on *Macrocystis pyrifera* Recruitment and Survival near Its Southern Limit off Baja California. *Botanica Marina*, *44*, 221–229.

Hobday, A. J., Alexander, L. V., Perkins, S. E., Smale, D. A., Straub, S. C., Oliver, E. C. J., ... Wernberg, T. (2016). A hierarchical approach to defining marine heatwaves. *Progress in Oceanography*, *141*, 227–238. <http://doi.org/10.1016/j.pocean.2015.12.014>

Howells, E. J., Beltran, V. H., Larsen, N. W., Bay, L. K., Willis, B. L., & van Oppen, M. J. H. (2012). Coral thermal tolerance shaped by local adaptation of photosymbionts. *Nature Clim. Change*, *2*(2), 116–120. Retrieved from <http://dx.doi.org/10.1038/nclimate1330>

Hurd, C., Harrison, P., Bischof, K., & Lobban, C. (2014). *Seaweed Ecology and Physiology*. <http://doi.org/10.1017/CBO9781139192637>

Jacox, M. G., Hazen, E. L., Zaba, K. D., Rudnick, D. L., Edwards, C. A., Moore, A. M., & Bograd, S. J. (2016). Impacts of the 2015-2016 El Niño on the California Current System: Early assessment and comparison to past events. *Geophysical Research Letters*, *43*(13), 7072–7080. <http://doi.org/10.1002/2016GL069716>

Johansson, M. L., Alberto, F., Reed, D. C., Raimondi, P. T., Coelho, N. C., Young, M. A., ... Serrão, E. A. (2015). Seascape drivers of *Macrocystis pyrifera* population genetic structure in the northeast Pacific. *Molecular Ecology*, *24*(19), 4866–4885. <http://doi.org/10.1111/mec.13371>

Joint, I., & Groom, S. B. (2000). Estimation of phytoplankton production from space: Current status and future potential of satellite remote sensing. *Journal of Experimental Marine Biology and Ecology*, *250*(1–2), 233–255. [http://doi.org/10.1016/S0022-0981\(00\)00199-4](http://doi.org/10.1016/S0022-0981(00)00199-4)

Jueterbock, A., Kollias, S., Smolina, I., Fernandes, J. M. O., Coyer, J. A., Olsen, J. L., & Hoarau, G. (2014). Thermal stress resistance of the brown alga *Fucus serratus* along the North-Atlantic coast: Acclimatization potential to climate change. *Marine Genomics*, *13*, 27–36. <http://doi.org/10.1016/j.margen.2013.12.008>

Kamykowsk, D. (1977). Latitudinal relationships among temperature and selected plant nutrients along the west coast of North and South America. *Journal of Marine Research*, *32*(2), 321–337.

Kirk, J. T. O. (2011). *Light and Photosynthesis in Aquatic Ecosystems*. (Cambridge University Press, Ed.).

Koch, K., Thiel, M., Hagen, W., Graeve, M., G??mez, I., Jofre, D., ... Bischof, K. (2016). Short- and long-term acclimation patterns of the giant kelp *Macrocystis pyrifera*

(Laminariales, Phaeophyceae) along a depth gradient. *Journal of Phycology*, 52(2), 260–273. <http://doi.org/10.1111/jpy.12394>

Ladah, L. B. (2003). The shoaling of nutrient-enriched subsurface waters as a mechanism to sustain primary productivity off Central Baja California during El Niño winters. *Journal of Marine Systems*, 42(3–4), 145–152. [http://doi.org/10.1016/S0924-7963\(03\)00072-1](http://doi.org/10.1016/S0924-7963(03)00072-1)

Ladah, L. B., Filonov, A., Lavinn, M. F., Leichter, J. J., Zertuche-Gonzalez, J. A., & Perez-Mayorga, D. M. (2012). Cross-shelf transport of sub-thermocline nitrate by the internal tide and rapid (3–6h) incorporation by an inshore macroalga. *Continental Shelf Research*, 42, 10–19. <http://doi.org/10.1016/j.csr.2012.03.010>

Ladah, L. B., & Zertuche-González, J. a. (2007). Survival of microscopic stages of a perennial kelp (*Macrocystis pyrifera*) from the center and the southern extreme of its range in the Northern Hemisphere after exposure to simulated El Niño stress. *Marine Biology*, 152(3), 677–686. <http://doi.org/10.1007/s00227-007-0723-z>

Lee, T., Awaji, T., Balmaseda, M. A., Greiner, E., & Stammer, D. (2009). Ocean State Estimation for Climate Research. *Oceanography*, 22(3), 162–167. <http://doi.org/10.5670/oceanog.2011.65>

Levine, A. F. Z., & Mcphaden, M. J. (2016). How the July 2014 Easterly Wind Burst Gave the 2015–16 El Niño a Head Start. *Geophysical Research Letters*, (July 2014). <http://doi.org/10.1002/2016GL069204>

Lichtenthaler, H. K., Buschmann, C., & Knapp, M. (2005). How to correctly determine the different chlorophyll fluorescence parameters and the chlorophyll fluorescence decrease ratio Rfd of leaves with the PAM fluorometer. *Photosynthetica*, 43(3), 379–393. <http://doi.org/10.1007/s11099-005-0062-6>

Lima, F. P., & Wethey, D. S. (2012). Three decades of high-resolution coastal sea surface temperatures reveal more than warming. *Nature Communications*, 3, 704. <http://doi.org/10.1038/ncomms1713>

Lomolino, M. V., Riddle, B. R., & Brown, J. H. (2006). Biogeography. In *Biogeography, Forth Edition* (pp. 10–11). http://doi.org/10.1007/SpringerReference_29469

Marbà, N., & Duarte, C. M. (2010). Mediterranean warming triggers seagrass (*Posidonia oceanica*) shoot mortality. *Global Change Biology*, 16(8), 2366–2375. <http://doi.org/10.1111/j.1365-2486.2009.02130.x>

McCullagh, P., & Nelder, J. A. (1989). *Generalized Linear Models, Second Edition*. <http://doi.org/10.1007/978-1-4899-3242-6>

McDonald, A. E., Ivanov, A. G., Bode, R., Maxwell, D. P., Rodermel, S. R., & Hüner, N. P. A. (2011). Flexibility in photosynthetic electron transport: The physiological role of plastoquinol terminal oxidase (PTOX). *Biochimica et Biophysica Acta - Bioenergetics*, 1807(8), 954–967. <http://doi.org/10.1016/j.bbabi.2010.10.024>

Mills, K., Pershing, A., Brown, C., Chen, Y., Chiang, F.-S., Holland, D. S., ... Wahle, R. A. (2013). Fisheries Management in a Changing Climate Lessons from the 2012 ocean Heat Wave in the Northwest Atlantic. *Oceanography*, 26(2), 191–195. <http://doi.org/10.5670/oceanog.2010.11.COPYRIGHT>

Mohring, M. B., Wernberg, T., Wright, J. T., Connell, S. D., & Russell, B. D. (2014). Biogeographic variation in temperature drives performance of kelp gametophytes during warming. *Marine Ecology Progress Series*, 513(October 2014), 85–96. <http://doi.org/10.3354/meps10916>

Mota, C. F., Engelen, A. H., Serrão, E. A., & Pearson, G. A. (2015). Some don't like it hot: Microhabitat-dependent thermal and water stresses in a trailing edge population. *Functional Ecology*, 29(5), 640–649. <http://doi.org/10.1111/1365-2435.12373>

Newman, M., Alexander, M. A., Ault, T. R., Cobb, K. M., Deser, C., Di Lorenzo, E., ... Smith, C. A. (2016). The Pacific decadal oscillation, revisited. *Journal of Climate*, 29(12), 4399–4427. <http://doi.org/10.1175/JCLI-D-15-0508.1>

Nicastro, K. R., Zardi, G. I., Teixeira, S., Neiva, J., Serrão, E. A., & Pearson, G. A. (2013). Shift happens: trailing edge contraction associated with recent warming trends threatens a distinct genetic lineage in the marine macroalga *Fucus vesiculosus*. *BMC Biology*, 11(1), 6. <http://doi.org/10.1186/1741-7007-11-6>

North, W. J. (1983). *Separating effects of temperature and nutrients*. California Institute of Technology, W. M. Keck Engineering Laboratories.

North, W. J., James, D. E., & Jones, L. G. (1993). History of kelp beds (*Macrocystis*) in Orange and San Diego Counties, California. In A. R. O. Chapman, M. T. Brown, & M. Lahaye (Eds.), *Fourteenth International Seaweed Symposium: Proceedings of the Fourteenth International Seaweed Symposium held in Brest, France, August 16--21, 1992* (pp. 277–283). Dordrecht: Springer Netherlands. http://doi.org/10.1007/978-94-011-1998-6_33

North, W. J., & Zimmerman, R. C. (1984). Influences of macronutrients and water temperatures on summertime survival of *Macrocystis* canopies. *Hydrobiologia*, 116/117, 419–424.

Nyman, M. A., Brown, M. T., Neushul, M., Harger, B. W. W., & Keogh, J. A. (1993). Mass

distribution in the fronds of *macrocystis pyrifera* from New Zealand and California. *Hydrobiologia*, 260–261(1), 57–65. <http://doi.org/10.1007/BF00049004>

Paolo, F. S., Fricker, H. A., & Padman, L. (2015). Volume loss from Antarctic ice shelves is accelerating. *Scientific Reports*, 348(6232), 327–331.

Pearson, G. A., Lago-Leston, A., & Mota, C. (2009). Frayed at the edges: Selective pressure and adaptive response to abiotic stressors are mismatched in low diversity edge populations. *Journal of Ecology*, 97(3), 450–462. <http://doi.org/10.1111/j.1365-2745.2009.01481.x>

Perkins, S. E. (2011). Biases and model agreement in projections of climate extremes over the tropical Pacific. *Earth Interactions*, 15(24), 1–36. <http://doi.org/10.1175/2011EI395.1>

Platt, T., Gallegos, C. L., & Harrison, W. G. (1980). Photoinhibition of photosynthesis in natural assemblages of marine phytoplankton. *Journal of Marine Research (USA)*. <http://doi.org/citeulike-article-id:3354339>

Poloczanska, E. S., Babcock, R. C., Butler, A., Hobday, A. J., Hoegh-Guldberg, O., Kunz, T. J., ... Richardson, A. J. (2007). *Climate Change and Australian Marine Life. Oceanogr Mar Biol Annu Rev* (Vol. 45). <http://doi.org/10.1201/9781420050943.ch8>

Raimondi, P. T., Reed, D. C., & Washburn, L. (2004). Effects of self-fertilization in the giant kelp, *Macrocystis pyrifera*. *Ecology*.

Ralph, P. J., & Gademann, R. (2005). Rapid light curves: A powerful tool to assess photosynthetic activity. *Aquatic Botany*, 82(3), 222–237. <http://doi.org/10.1016/j.aquabot.2005.02.006>

Raven, J. A., & Geider, R. J. (1988). Temperature and algal growth. *New Phytologist*, 110(4), 441–461. <http://doi.org/10.1111/j.1469-8137.1988.tb00282.x>

Reed, D., Washburn, L., Rassweiler, A., Miller, R., Bell, T., & Harrer, S. (2016). Extreme warming challenges sentinel status of kelp forests as indicators of climate change. *Nature Communications*, 7(May), 13757. <http://doi.org/10.1038/ncomms13757>

Repolho, T., Duarte, B., Dionísio, G., Paula, J. R., Lopes, A. R., Rosa, I. C., ... Rosa, R. (2017). Seagrass ecophysiological performance under ocean warming and acidification. *Scientific Reports*, 1–12. <http://doi.org/10.1038/srep41443>

Ridgway, K. R. (2007). Long-term trend and decadal variability of the southward penetration of the East Australian Current. *Geophysical Research Letters*, 34(13), 1–5. <http://doi.org/10.1029/2007GL030393>

Rodriguez, G. E., Reed, D. C., & Holbrook, S. J. (2016). Blade life span, structural

investment, and nutrient allocation in giant kelp. *Oecologia*, 182(2), 397–404. <http://doi.org/10.1007/s00442-016-3674-6>

Roleda, M. Y., Campana, G. L., Wiencke, C., Hanelt, D., Quartino, M. L., & Wulff, A. (2009). Sensitivity of antarctic urospora penicilliformis (ulotrichales, chlorophyta) to ultraviolet radiation is life-stage dependent. *Journal of Phycology*, 45(3), 600–609. <http://doi.org/10.1111/j.1529-8817.2009.00691.x>

Rosenzweig, C., & Neofotis, P. (2013). Detection and attribution of anthropogenic climate change impacts. *Wiley Interdisciplinary Reviews: Climate Change*, 4(2), 121–150. <http://doi.org/10.1002/wcc.209>

Rothausler, E., Gomez, I., Hinojosa, I., Karsten, U., Tala, F., & Thiel, M. (2009). Effect of Temperature and Grazing on Growth and Reproduction of Floating *Macrocystis* Spp. (Phaeophyceae) Along a Latitudinal Gradient. *Journal of Phycology*, 45, 547–559. <http://doi.org/10.1111/j.1529-8817.2009.00676.x>

Sakshaug, E., Bricaud, A., Dandonneau, Y., Falkowski, P. G., Kiefer, D. a, Legendre, L., ... Takahashi, M. (1997). Parameters of photosynthesis: definitions, theory and interpretation of results. *Journal of Plankton Research*, 19(11), 1637–1670. <http://doi.org/10.1093/plankt/19.11.1637>

Santelices, B., & Ojeda, F. (1984). Effects of canopy removal on the understory algal community structure of coastal forests of *Macrocystis pyrifera* from southern South America. *Marine Ecology Progress Series*, 14(August), 165–173. <http://doi.org/10.3354/meps014165>

Schmitz, K., & Grant, A. (1979). Long Distance Transport in *Macrocystis integrifolia*. *Plant Physiology*, 63, 995–1002.

Selig, E. R., Casey, K. S., & Bruno, J. F. (2010). New insights into global patterns of ocean temperature anomalies: Implications for coral reef health and management. *Global Ecology and Biogeography*, 19(3), 397–411. <http://doi.org/10.1111/j.1466-8238.2009.00522.x>

Smale, D. A., & Wernberg, T. (2012). Ecological observations associated with an anomalous warming event at the Houtman Abrolhos Islands, Western Australia. *Coral Reefs*, 31(2), 441. <http://doi.org/10.1007/s00338-012-0873-4>

Switzer, A. C., Kamykowski, D., & Zentara, S. J. (2003). Mapping nitrate in the global ocean using remotely sensed sea surface temperature. *Journal of Geophysical Research Oceans*, 108(C8), NIL_1-NIL_12. <http://doi.org/10.1029/2000JC000444>

Tamburic, B., Guruprasad, S., Radford, D. T., Szabó, M., Lilley, R. M. C., Larkum, A. W. D., ... Ralph, P. J. (2014). The effect of diel temperature and light cycles on the growth of

Nannochloropsis oculata in a photobioreactor matrix. *PLoS ONE*, 9(1). <http://doi.org/10.1371/journal.pone.0086047>

Terada, R., Vo, T. D., Nishihara, G. N., Shioya, K., Shimada, S., & Kawaguchi, S. (2016). The effect of irradiance and temperature on the photosynthesis and growth of a cultivated red alga *Kappaphycus alvarezii* (Solieriaceae) from Vietnam, based on in situ and in vitro measurements. *Journal of Applied Phycology*, 28(1), 457–467. <http://doi.org/10.1007/s10811-015-0557-x>

Tietsche, S., Balmaseda, M. A., Zuo, H., & Mogensén, K. (2015). Arctic sea ice in the global eddy-permitting ocean reanalysis ORAP5. *Climate Dynamics*, (737), 33. <http://doi.org/10.1007/s00382-015-2673-3>

Trenberth, K. E. (2012). Framing the way to relate climate extremes to climate change. *Climatic Change*, 115(2), 283–290. <http://doi.org/10.1007/s10584-012-0441-5>

Wernberg, T., de Bettignies, T., Joy, B. A., & Finnegan, P. M. (2016). Physiological responses of habitat-forming seaweeds to increasing temperatures. *Limnology and Oceanography*, 61(6), 2180–2190. <http://doi.org/10.1002/lno.10362>

Wernberg, T., Smale, D. A., & Thomsen, M. S. (2012). A decade of climate change experiments on marine organisms: Procedures, patterns and problems. *Global Change Biology*, 18(5), 1491–1498. <http://doi.org/10.1111/j.1365-2486.2012.02656.x>

Wernberg, T., Smale, D. a., Tuya, F., Thomsen, M. S., Langlois, T. J., de Bettignies, T., ... Rousseaux, C. S. (2012). An extreme climatic event alters marine ecosystem structure in a global biodiversity hotspot (Supplementary information). *Nature Climate Change*, 3(1), 78–82. <http://doi.org/10.1038/nclimate1627>

Wernberg, T., Thomsen, M. S., Tuya, F., Kendrick, G. A., Staehr, P. A., & Toohy, B. D. (2010). Decreasing resilience of kelp beds along a latitudinal temperature gradient: Potential implications for a warmer future. *Ecology Letters*, 13(6), 685–694. <http://doi.org/10.1111/j.1461-0248.2010.01466.x>

Westermeier, R., Patiño, D., Piel, M. I., Maier, I., & Mueller, D. G. (2006). A new approach to kelp mariculture in Chile: Production of free-floating sporophyte seedlings from gametophyte cultures of *Lessonia trabeculata* and *Macrocystis pyrifera*. *Aquaculture Research*, 37(2), 164–171. <http://doi.org/10.1111/j.1365-2109.2005.01414.x>

Wheeler, P. A., & North, W. J. (1980). Effect of Nitrogen Supply on Nitrogen Content and Growth Rate of Juvenile *Macrocystis Pyrifera* (Phaeophyta) Sporophytes. *Journal of Phycology*, 16, 577–582. <http://doi.org/10.1111/j.1529-8817.1980.tb03076.x>

Xu, D., Ye, N., Cao, S., Wang, Y., Wang, D., Fan, X., ... Mao, Y. (2013). Variation in morphology and PSII photosynthetic characteristics of *Macrocystis pyrifera* during development from gametophyte to juvenile sporophyte. *Aquaculture Research*, n/a-n/a. <http://doi.org/10.1111/are.12327>

Zimmerman, R. C., & Kremer, J. N. (1984). Episodic nutrient supply to a kelp forest ecosystem in Southern California. *Journal of Marine Research*, 42(3), 591–604. <http://doi.org/10.1357/002224084788506031>

Zuo, H., & Balmaseda, M. A. (2015). The ECMWF-MyOcean2 eddy-permitting ocean and sea-ice reanalysis ORAP5. Part 1: Implementation. *ECMWF Technical Memoranda*, 736(February), 1–42.

Zuo, H., Balmaseda, M. A., & Mogensen, K. (2015). The new eddy-permitting ORAP5 ocean reanalysis: description, evaluation and uncertainties in climate signals. *Climate Dynamics*, 1–21. <http://doi.org/10.1007/s00382-015-2675-1>

Annexes

Annex I: Sampling sites (populations) and coordinates per region

Region	Population name	Coordinates
North	Mitchell's Cove	36° 56.896' N 122°02.066' W
	Pleasure Point	36° 57.094' N 121°58.723' W
North-Center	Santa Barbara 1	34° 24.345' N 119° 52.301' W
	Santa Barbara 2	34° 23.469' N 119° 32.515' W
South-Center	Campo Kennedy	31°42'00.5"N 116°40'52.7"W
	Arbolitos	31°42'46.8"N 116°42'25.6"W
South	Punta Eugenia	27°50'58.3"N 115°04'57.6"W
	Bahia Tortugas	27°39'51.7"N 114°54'14.4"W

Annex II: Tukey Honest Significant Differences (HSD) of generalized linear models (GLMs) comparison between the interaction Temperature x Nutrients reported on Table 3 on the variables maximum quantum yield of PSII (F_v/F_m) on the 2nd experiment and mean F_v/F_m values of contrasts. Significant p-values are marked in bold.

Contrasts						Mean	Mean
1	2	diff	lower	upper	p-value	F_v/F_m 1	F_v/F_m 2
24°C Enriched	x 16°C Enriched	-0.02142	-0.03377	-0.00907	5.69E-05	0.727	0.762
				0.00534			
16°C Non-enriched	x 16°C Enriched	-0.00246	-0.01027	9	0.848562	0.758	0.762
24°C Non-enriched	x 16°C Enriched	-0.0561	-0.06845	-0.04375	0	0.674	0.762
			0.00660				
16°C Non-enriched	x 24°C Enriched	0.018959	7	0.03131	0.000503	0.758	0.727
24°C Non-enriched	x 24°C Enriched	-0.03468	-0.0503	-0.01906	1E-07	0.674	0.727
24°C Non-enriched	x 16°C Non-enriched	-0.05364	-0.06599	-0.04129	0	0.674	0.758